

Review

# Gold and Platinum Group Element Occurrence Related to Black Shale Formations in the Southern Urals (Russia): A Review

Alexander V. Snachev <sup>1,\*</sup>  and Mikhail A. Rassomakhin <sup>2</sup> 

<sup>1</sup> Institute of Geology Ufa Federal Research Centre of the Russian Academy of Sciences, Karl Marks Str., 16/2, 450077 Ufa, Russia

<sup>2</sup> South Urals Federal Research Center of Mineralogy and Geoecology of the Ural Branch Russian Academy of Sciences, 456317 Miass, Russia; miha\_rassomahin@mail.ru

\* Correspondence: savant@rambler.ru

**Abstract:** This paper gives a brief description of all structural–formational zones in the Southern Urals. Riphean and Paleozoic black shale sediments with strong positive anomalies of gold and a number of other elements are widely developed within this region. This paper reports that carbonaceous shales are a very favorable geochemical environment for the primary accumulation of many industrially important elements. Under certain conditions (in the areas of magmatism, zonal metamorphism, and tectonic activity), they can serve as a source of metals and concentrate deposits, and occurrences of gold, silver, and platinum. Among these deposits, a new type of vein-embedded gold–sulfide mineralization with dispersed gold and platinum metals, localized in rocks rich in organic carbon, has been detected. In this study, we made an attempt to summarize and systematize research materials on this issue. The presented data indicate a high potential of carbonaceous sediments in the Southern Urals, providing a good basis for further prospecting works and analytical studies.

**Keywords:** Southern Urals; black shales; carbonaceous shales; gold; platinum group elements; silver; sulfides; gold deposits



**Citation:** Snachev, A.V.; Rassomakhin, M.A. Gold and Platinum Group Element Occurrence Related to Black Shale Formations in the Southern Urals (Russia): A Review. *Minerals* **2024**, *14*, 1283. <https://doi.org/10.3390/min14121283>

Academic Editor: Maria Economou-Eliopoulos

Received: 8 November 2024

Revised: 6 December 2024

Accepted: 10 December 2024

Published: 17 December 2024



**Copyright:** © 2024 by the authors. Licensee MDPI, Basel, Switzerland. This article is an open access article distributed under the terms and conditions of the Creative Commons Attribution (CC BY) license (<https://creativecommons.org/licenses/by/4.0/>).

## 1. Introduction

Carbonaceous sediments are known to be a very favorable geochemical environment for the primary accumulation of many industrially important elements. In certain conditions, especially in the areas of magmatism, zonal metamorphism, and tectonic activity, carbonaceous rocks can concentrate large deposits of gold, molybdenum, tungsten, vanadium, manganese, platinum, and other elements. Examples include large deposits of gold and platinum such as Broken Hill, Muruntau, and Sukhoi Log [1–12].

Currently developed geological and genetic models of gold formation, including those in black shale formations, suggest the complex participation of interrelated processes of sedimentation, tectonics, magmatism, and metamorphism in orogenesis, with one or more of them playing a leading role [13–16].

The prevailing view among foreign researchers is the key role of metamorphogenic fluids in the formation of ore mineralization in carbonaceous complexes [9,17,18]. Russian scientists believe that they have a polygenetic and polychronic nature [19–22]. The probable generation mechanism of fluids, which is responsible for the polygenetic character of mineralization, was suggested by N.S. Bortnikov and coauthors [23,24]. Nowadays, researchers are mostly focused on the study of the composition and sources of mineral-forming fluids, using the methods of thermobarochemistry, gas chromatography, and geochemical isotope analysis of minerals of gold ores [25–30]. According to the results of studies on gold deposits and occurrences located in carbonaceous sediments, the proposed model of gold formation can be regarded as sedimentary, hydrothermal, and metamorphogenic, including the following characteristics [31–46]: (1) sedimentation with chemogenic sorption of gold by carbonaceous–clay sediments; (2) immersion metamorphism, activation

of elision pore solutions that extract ore elements and gold from the clay fraction, their redistribution and mobilization in collector beds (carbonaceous–sulfide sediments as geochemical barriers), and the production of intermediate above-background concentrations; (3) dynamo-metamorphism, thrusting, and folding, accompanied by the metamorphogenic rearrangement and redeposition of mineral matter; and (4) contact and zonal metamorphism during the formation of granite–migmatite domes, dike complexes, large intrusive granitoid massifs, and the complete “formation” of ore deposits in their present form.

Many researchers have reported that during metasomatism and sulfidization processes, the migration of gold takes place [47–54]. The mechanism of its concentration is most clearly manifested when higher stages of regional, contact, and dislocation metamorphism are superimposed on carbon-bearing sediments [9]. In particular, through examples of Siberian and Far Eastern [31,55–58] gold deposits and occurrences, as well as Southern Ural objects [59,60], they show that gold–sulfide mineralization occurs in the high-temperature subfacies of greenschist facies, which are considered zones of gold deposition, while higher-temperature facies are considered zones of potential removal. It is in this geological setting that zones of sulfidized carbonaceous rocks and large quartz vein fields, which are worth assessing for gold content, have been found within the Southern Urals [61–65].

For many years, all exploration work in the Southern Urals was focused on traditional types of noble metals. Currently, the situation has changed somewhat, leading to the discovery of a number of objects with vein-disseminated gold–sulfide mineralization and dispersed gold, platinum, and rare metals in the deposits of black shale formations [59,62,66,67]. In this paper, we provide an overview of a number of Southern Ural gold ore occurrences studied by various authors, occurring in carbonaceous deposits framing granite–gneiss domes or in the immediate vicinity of large granite massifs and faults.

## 2. Materials and Methods

The main volume of analytical studies on carbonaceous shales for gold and 4 elements of the platinum group (platinum, palladium, rhodium, and iridium) was carried out in the Institute of Geology of Ore Deposits, Petrography, Mineralogy, and Geochemistry of the Russian Academy of Sciences (IGEM RAS, Moscow) in the laboratory for “Mineral Matter Analysis” (Head of the Laboratory, V.V. Distler). In total, more than 450 pit and trench samples were analyzed. Samples weighing 300–400 g were crushed and quartered to a 100 g weight. The analyses were performed using the atomic absorption method with chemical–spectral termination and a thermal atomizer [68]. This included three stages: the decomposition of the sample, the separation of the concentrate on the graphite collector, and the determination of platinum metal contents on the collector. The lower limits of quantitative determinations (g/t) were the following: Pt—0.02; Pd—0.03; Rh and Ir—0.01; and Au—0.05. The laboratory conducted similar works in the largest Sukhoi Log gold deposit, certified by the State Standard of Russia [58,69–71].

In addition, about 80 samples of carbonaceous shale were analyzed for Au, Pt, and Pd following the fire assay procedure in the Analytical Center of the Central Research Geological Exploration Institute of Nonferrous and Noble Metals (FGUP TSNIGRI, Moscow) (Head of Department, A.V. Mandrugin). The fire assay procedure is widely used in analytical practice and is often considered a reference method for the precise determination of gold content in rocks with an uneven distribution of noble metals [72,73]. The sample for the analysis weighed about 50 g. At the first stage, the sample was charged and followed by crucible melting at temperatures of 1050–1100 °C and cupellation to silver (0.01 g) or lead (0.1 g) bead. The samples were analyzed using quantitative mass spectrometry with chemical concentration (measured using the Perkin Elmer ELAN 6100). The lower limit of quantitative determination of elements was (g/t) Au—0.005, Pt—0.002, Pd—0.002, and Rh—0.0005 [74].

The photographs of the surface of gold particles and microprobe analysis were made on a Tescan Vega 3 scanning electron microscope with an Oxford Instruments X-act energy dispersive spectrometer in the Federal State Budgetary Institution of Science South Urals

Research Center of Mineralogy and Geocology of the Urals Branch of the Russian Academy of Sciences (analyst M.A. Rassomakhin, carbon coating was used, accelerating voltage was 20 kV, “live” time was 120 s, MAC standards—Micro-Analysis Consultants LTD, reg. No. 1362).

### 3. Geology and Gold Content of Carbonaceous Sediment

The South Ural fold system is a series of successively alternating paleocontinental and paleoceanic submeridional structural formation zones (from west to east: Bashkir Meganticlinorium, Zilair Megasyntlinorium, Uraltau Meganticlinorium, Magnitogorsk Megasyntlinorium, Aramil–Sukhtelinsk Synclinorium, East Ural Megazone, Uray–Denisovka Zone) (Figure 1).

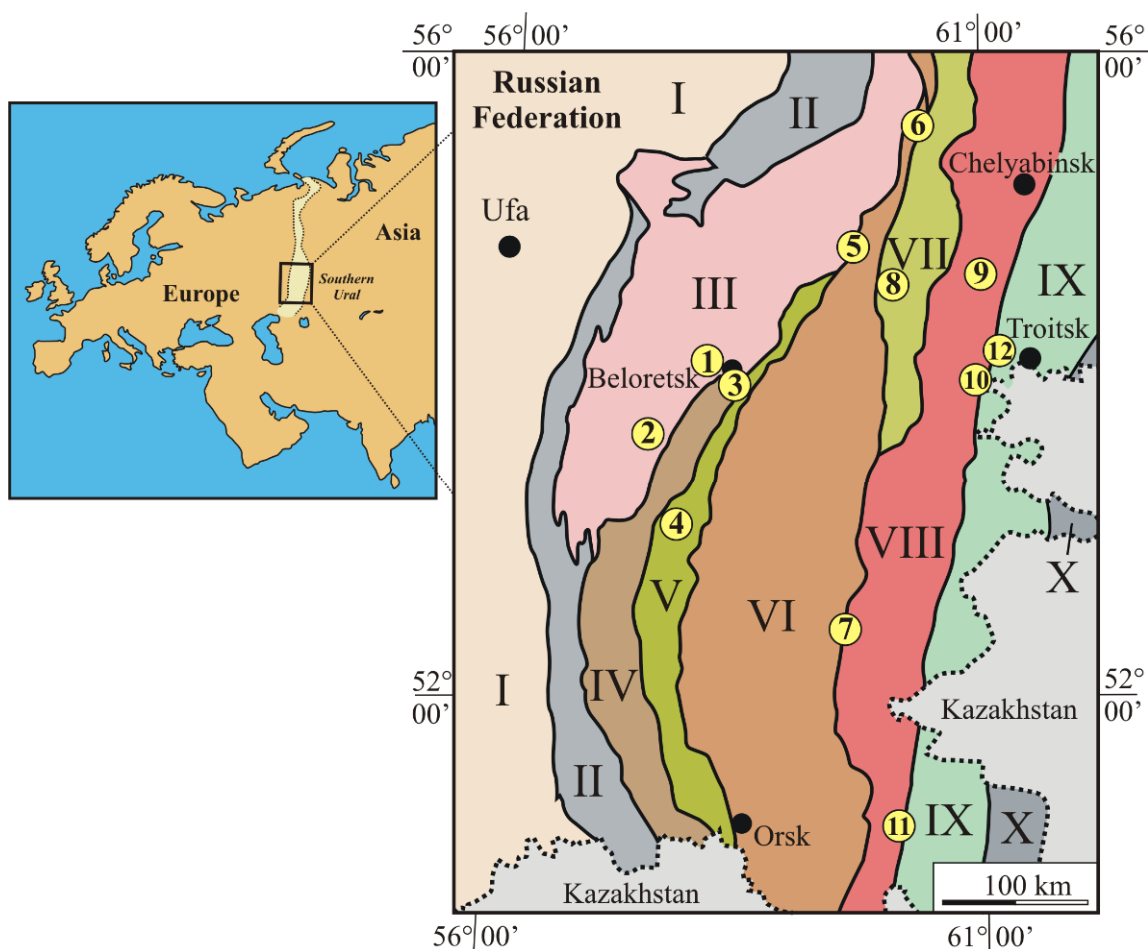


**Figure 1.** Tectonic zoning scheme of the Southern Urals and objects mentioned in the article. Structural formational zones (Yu. G. Knyazev et al. [75], simplified by the authors): I—East European Platform, II—Cis-Ural foredeep, III—Bashkirian Meganticlinorium, IV—Zilair Synclinorium, V—Uraltau Meganticlinorium, VI—Magnitogorsk Megasyntlinorium, VII—Aramil–Sukhtelinsk Synclinorium, VIII—East Ural Megazone, IX—Trans-Ural Uplift, X—Uray–Denisovka Zone. Numbers in circles represent gold occurrences: 1—Otnurok, 2—Gorny Priisk, 3—Yatva section, 4—Novousmano area, 5—Siratur ore field, 6—Chernoe Ozero occurrence, 7—Amur deposit, 8—Larino dome, 9—Tetechnaya Mountain, 10—Kamenka area, 11—Kumak ore field, 12—Belokamenka and Osipovka areas.

Each of these zones underwent particular stages of geodynamic development (continental riftogenic, oceanic, island arc, active continental margin, collisional, and tectono-magmatic activation). Gold deposits and occurrences bound to carbonaceous rocks of different ages and genetic and formational types are known in all of them.

### 3.1. Bashkirian Meganticlinorium

The Beloretsk zonal metamorphic complex is localized in the eastern part of the Bashkirian Meganticlinorium. It bends around the northern closure of the Zilair Synclinorium in a horseshoe shape and extends in the northeastern direction for a distance of about 120 km with a width of 20 to 40 km (Figure 2). It is composed of the Lower–Middle and Upper Riphean sediments, the total thickness of which ranges from 4 to 5 km [61,76].

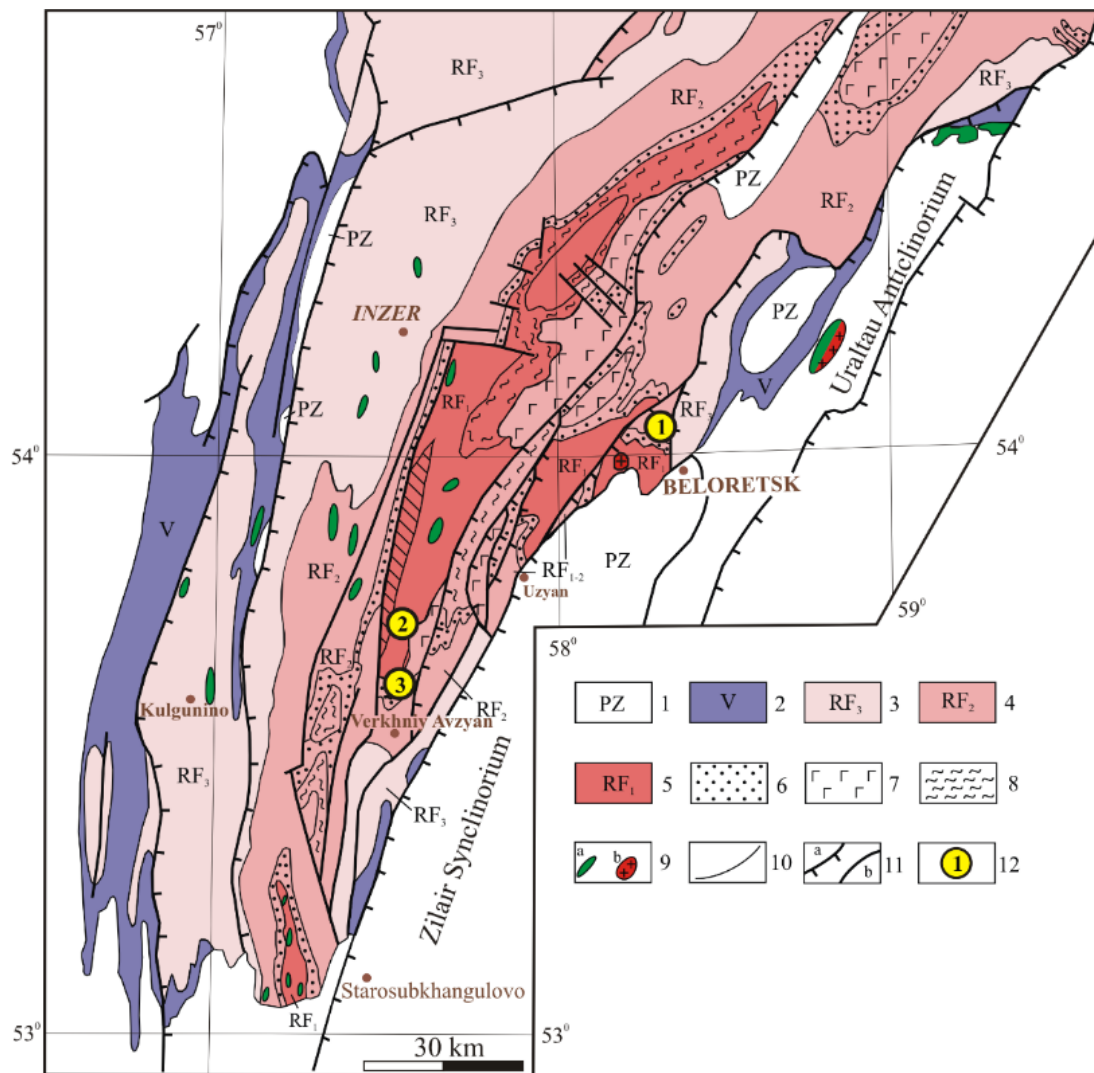


**Figure 2.** Schematic geological map of Bashkirian Meganticlinorium [61]. Legend: 1—unsubdivided deposits of Paleozoic, 2—unsubdivided deposits of Vendian, 3—unsubdivided deposits of Upper Riphean, 4—Zygazino–Komarovskiy and Avzyan Formations, 5—unsubdivided deposits of Lower Riphean, 6—Zygalga Formation, 7—Mashak Formation, 8—Bakal and Jusha Formations, 9—magmatic formations: gabbro–dolerites (a), granites (b), 10—geological boundaries, 11—main faults: a—thrusts, b—normal faults, 12—gold occurrences: 1—Otnurok, 2—Ulyuk Bar, 3—Gorny Priisk.

The source rocks for the Beloretsk metamorphic complex are predominantly sand–clay and carbonate sediments with rather thick interlayers of carbonaceous formations, much less frequent intrusive bodies, and effusions of basic composition. As a result of metamorphism, a zonal complex was formed, the central part of which (7–8 km in diameter) is composed of eclogite facies of metamorphism, the intermediate part (2–10 km wide) is compared of amphibolite facies, and the outer part is composed of greenschist facies (15–20 km wide). A.A. Alekseev et al. [76] report that the studies of plagioclase–hornblende, garnet–biotite, garnet–amphibole, and other thermobarometers showed that the rocks of eclogite, amphibolite

and greenschist facies of metamorphism were formed, respectively, under the following PT-conditions: 12–13 kbar and 600–650 °C; 5.0–5.5 kbar and 500 °C; and 2–3 kbar and 350–400 °C. A small granitoid massif observed on the surface occurs as a series of small outcrops of gneiss-like and metamorphosed granites (Akhmerov Massif), the age of which from the latest data is estimated at  $1381 \pm 23$  Ma [77], and thus it has no direct relation to the formation of the described metamorphic zonality.

Within the Beloretsk complex, carbonaceous sediments are developed in the Jusha, Mashak, Zigalga, and Zigazino–Komarovsky Formations [59]. Carbonaceous shales are most widespread in the Zigazino–Komarovsky Formation (RF<sub>2</sub>zk). It is composed, in varying ratios, of chlorite–sericite–quartz, micaceous–quartz, micaceous–feldspar–quartz shales, quartz siltstones, and sandstones enriched with carbonaceous matter, and by their petrochemical features, they belong to the terrigenous–carbonaceous formation. Sulfidization from single disseminated pyrite grains leads to the formation of up to 1 cm thick sulfide veins with sulfide content in rocks up to 25%–30% and is frequently observed in the shales (Figure 3).

We have collected the available material on the noble metal ore content of carbonaceous sediments of the Beloretsk metamorphic complex and carried out about 200 analyses of our own pit and trench samples [63,78], some of which are presented in Table 1.

In spite of the relatively small number of analyzed samples, the data obtained suggest a high prospectivity of carbonaceous sediments of the Zigazino–Komarovsky Formation. Thus, the average gold content of its 21 samples was 0.29 g/t, which corresponds to the ore anomaly. The maximum contents of gold in the samples of carbonaceous shales of the Zygazino–Komarovsky Formation reach 2.05 g/t in a small quarry near the road between Beloretsk and Otnurok settlement (Figure 3). In the interval of 15.5–17.0 m in the quarry, there is a layer of intensely dislocated carbonaceous shales, in which isolated lenses or thin interbedding of silicified brown ironstones were noticed. Analysis of the layers with a 0.5 m long furrow showed 3.43 g/t gold, which allows us to propose this area for further exploration.

**Table 1.** Contents of noble elements in the sediments of the Beloretsk complex (g/t) [59,63].

No.	Sample	Au	Pt	Pd	Rh	Ir	No.	Sample	Au	Pt	Pd	Rh	Ir
1	7247	0.760	–	0.060	0.007	0.008	16	7111-2	0.111	0.064	0.027	–	0.006
2	7134-1	0.280	–	0.055	0.008	0.050	17	5348	0.005	0.004	–	0.001	0.014
3	7126-1	0.019	–	0.083	0.008	0.028	18	5814-1	0.081	0.006	0.010	0.011	0.028
4	7237/1	0.230	0.023	0.160	0.007	0.008	19	5386-1	0.046	0.002	0.009	0.004	0.027
5	7127	0.089	0.033	0.098	0.005	–	20	7010-1	0.018	0.020	0.027	–	0.038
6	7244	–	0.004	0.210	0.006	–	21	7011-3	1.680	0.003	0.032	–	0.026
7	7233	–	–	0.110	0.003	–	22	7084-1	0.054	0.083	0.032	–	0.064
8	7241	0.260	0.010	0.035	0.003	–	23	5932	0.210	0.012	0.014	–	0.008
9	7094	1.420	0.041	0.019	–	0.010	24	5848-2	0.100	–	0.270	0.004	–
10	7094-1	0.130	0.038	0.037	–	0.019	25	7128	0.033	0.016	0.086	–	0.013
11	7095	0.061	0.011	0.015	–	0.006	26	5859-2	0.035	0.006	0.009	0.034	0.005
12	7123	0.075	0.009	0.054	–	0.011	27	5862	0.051	–	0.890	0.008	0.034
13	7131	0.470	0.025	0.010	–	–	28	5878-2	0.038	0.003	0.480	0.003	0.019
14	7136-1	0.070	0.038	0.111	–	0.012	29	5861	0.030	0.002	0.075	0.006	0.090
15	7134-1	2.050	0.056	0.046	–	0.016	30	5878-3	0.020	–	0.033	0.013	–

Note: Formations: 1–15—Zigazino–Komarovsky, 16–23—Mashak, 24–25—Ayusapkan, 26–30—Kyzyltash. Nos. 1, 8, 23—brown ironstone; No. 21—sandstone; No. 28—quartz vein, the rest—carbonaceous shales. Dash—content of the element is below the sensitivity threshold of the analysis. The analysis was carried out at IGEM RAS (Moscow).

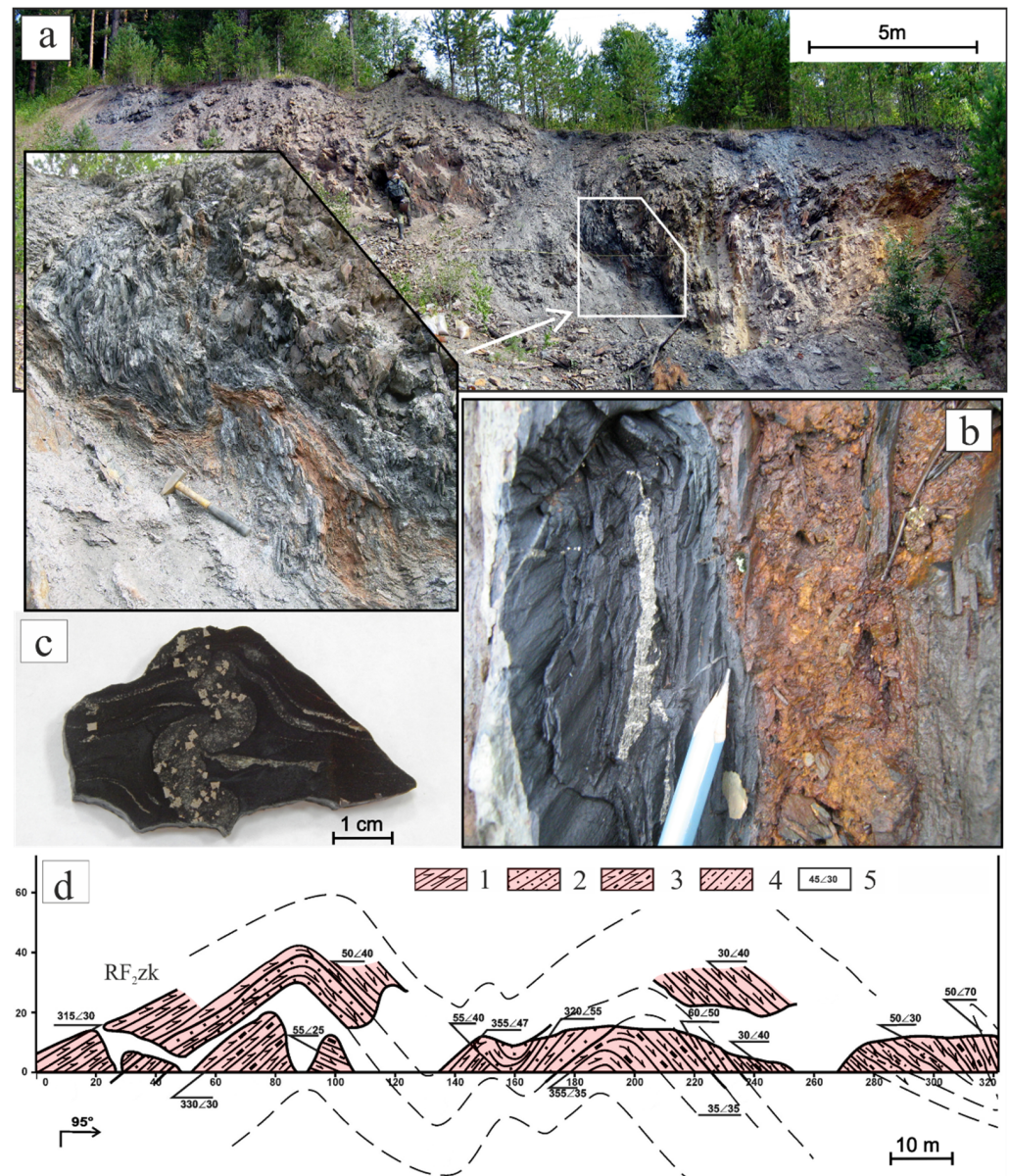


**Figure 3.** Photos of sections of the Zygazino–Komarovsky Formation (a), sulfide mineralization in black shales (b,c), a section of intensely dislocated shales (Otnurok occurrence), and (d): 1—muscovite–quartz shale, 2—sandstone, 3—calcareous muscovite–quartz shale, 4—quartz siltstone, 5—bedding elements.

In the western end of the Beloretsk metamorphic complex, there are a number of primary deposits and gold occurrences and deposits confined to the Riphean terrigenous strata, such as Gorny Priisk, Ulyuk–Bar, Kalashnikova vein, Bogryashka, Rameeva vein, Kurgashlinskoye, along with the above placers form the Avzyan ore and placer knot (Figures 2 and 4) [67,79–83]. The Gorny Priisk deposit is the most promising of them and is confined to the tectonic block bounded on the east and west by the Karatash and Bolsheavzyan faults of the submeridional strike. It is localized in the terrigenous–carbonaceous sediments of the Zygazino–Komarovsky Formation (RF<sub>2</sub>zk). The ore bodies are of three types: strata, veins, and veinlets. Tabular ore bodies are represented by sulfide phenocrysts in the schist formation zones of carbonaceous shales and sandstones. The vein type is represented by gold-bearing carbonate–quartz veins in the zones of shale formation and fractures. The vein ore bodies are composed of quartz veins with phenocrysts of pyrite and chalcopyrite.

Sampling of light-gray weakly carbonaceous shales and quartz veins within the ore zone of the deposit showed rather stable contents of gold, typically no higher than 2–4 g/t. In

the sulfide-rich interveins (pyrite up to 20%–40%) and in the areas that underwent tectonic reworking and hydrothermal alteration, the contents sharply increase to tens of g/t [59] (Table 2). The linear-planar weathering crust is widely developed at the deposit in the zone of crushing and mineralization. In 2001, the sample material of the gold-bearing weathering crust of the Gorny Priisk ore field was studied using the technology of in situ hypochloride leaching and recognized as suitable for mining with this procedure [84,85].

The native gold of the Gorny Priisk deposit is mostly fine, up to 0.1 mm in size, and is of high fineness (955–980) [86]. In morphology, it is represented mainly by sponge and dendrite forms, which positively influences its dissolution during leaching (Figure 4). The main impurity is silver, the content of which is in the range of 3–5 wt.%, rarely reaching 13 wt.%. Small amounts of Bi (up to 1.2 wt.%), As (0.7 wt.%), Sb, Se, Te, and Ni (0.2–0.3 wt.%) are observed. In the pits, on the surface of gold particles, numerous films and coatings of iron oxides and hydroxides, as well as a large number of microparticles of very high fineness gold to 0.1–0.5 microns in size and dendrites of newly formed gold up to 10 microns in size, were found (Figure 4). Nanogold is preserved in the grooves and microcracks of the surface of the gold particles. Its detection in large quantities on the surface of the gold grains serves as an indicator of the ongoing redistribution processes of ore substance [87].

Analysis and generalization of the results of analytical studies allow us to conclude that all gold occurrences with high gold contents (Otnurok, Kudashmanovo, Ulu–Yelga, Ishlya, Kagarmarovo, Gadylshino, high contents at Shirokaya Mountain, Mayardak Ridge, etc.) belong to the area of epidote–amphibolite or greenschist facies of metamorphism (Figure 5).

Ore mineralization is observed throughout the thickness of the section, but its intensity typically increases in the areas of increased stratification and crushing of host rocks. Here, one can observe sulfidized and silicified zones of shatter and crush, quartz veins, and stockwork zones bordering the wings and curves of folds [63,78,88].

The sulfide-disseminated type of mineralization has a distinct lithological and structural control—an obvious selective confinement to carbonaceous sediments localized in the near-fault zone of the intense dislocation of rocks. The comparative simplicity of mineral composition, the absence of contrasting areas of hydrothermal changes, and typical dynamo-metamorphogenic regeneration textures of rocks indicate a wide participation of dislocation metamorphism processes in the formation of quartz–sulfide mineralization.

**Table 2.** Contents of Au and Ag in silicified and ferruginated black shales and sandstones of the Gorny Priisk deposit (g/t).

No.	Sample	Au	Ag	No.	Sample	Au	Ag	No.	Sample	Au	Ag
1	GP-1	1.8	6.8	15	GP-17	0.1	4.1	29	GP-29	5.8	5.8
2	GP-2	0.9	7.4	16	GP-18	0.1	6.1	30	GP-30	0.4	7.0
3	GP-3	8.8	9.2	17	GP-19	11.4	4.2	31	GP-31	0.8	8.2
4	GP-5	0.4	1.8	18	GP-20	0.8	4.2	32	GP-32	2.5	8.5
5	GP-7	0.1	3.1	19	GP-21	1.6	5.8	33	GP-33	0.4	5.0
6	GP-8	0.2	10.8	20	GP-22	2.0	5.8	34	GP-34	0.2	1.8
7	GP-9	0.6	5.8	21	GP-23	0.2	4.8	35	GP-35	0.1	5.3
8	GP-10	0.6	2.2	22	GP-24	1.1	18.3	36	GP-36	0.4	6.8
9	GP-11	0.3	4.1	23	GP-25	0.1	25.3	37	GP-37	0.3	8.8
10	GP-12	2.6	5.4	24	GP-26/1	5.5	101.8	38	GP-38	0.2	5.2
11	GP-13	0.7	8.9	25	GP-26/2	0.4	8.2	39	GP-49	0.2	0.4
12	GP-14	0.1	4.1	26	GP-27/1	0.8	51.6	40	GP-52	9.1	0.1
13	GP-15	0.2	4.2	27	GP-27/2	1.0	4.6	41	GP-54	0.3	0.1
14	GP-16	0.4	4.6	28	GP-28	0.2	12.4	42	GP-55	4.9	0.1

Note: analyses were performed at the Analytical Laboratory of Mindyak mine by the fire assay procedure (analyst N.M. Kirsanova).

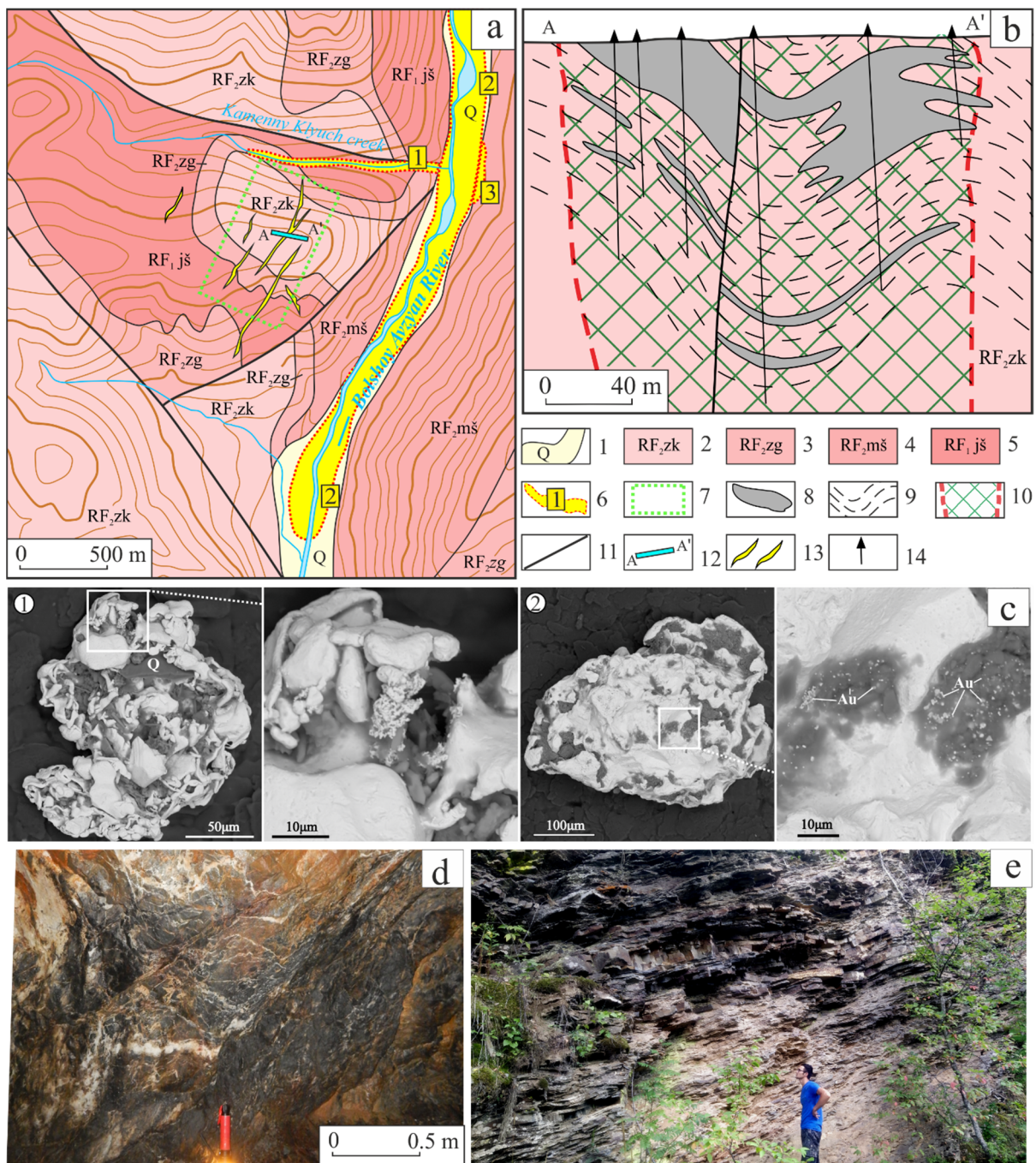


**Figure 4.** Geologic map (a) and cross-section (b) [86] of the Gorny Priisk deposit: 1—Quaternary deposits, 2—Zigazino–Komarovskiy Formation (carbonaceous–clayey shales, sandstones), 3—Zigalga Formation (sandstones, quartzite sandstones), 4—Mashak Formation (meta-sandstones, basalt lavas), 5—Jusha Formation (clayey siltstones, sandstones), 6—placer contours and their numbers (1—Kamenny Klyuch, 2—Avzyan, 3—Shatak Bort), 7—Gorny Priisk deposit contour, 8—gold-bearing sandy shale deposits, 9—carbonaceous–clayey shales, 10—oxidation and tectonic reworking zone, 11—faults, 12—position of the cross-section A–A', 13—gold-bearing quartz veins, 14—exploratory wells; electron microscopic images of native gold from the weathering crust: (1) dendrites of newly formed gold, (2) nanogold in the surface of the gold particles (c), quartz veins in carbonaceous shales, (d) and interbedded sandstones and black shales (e).

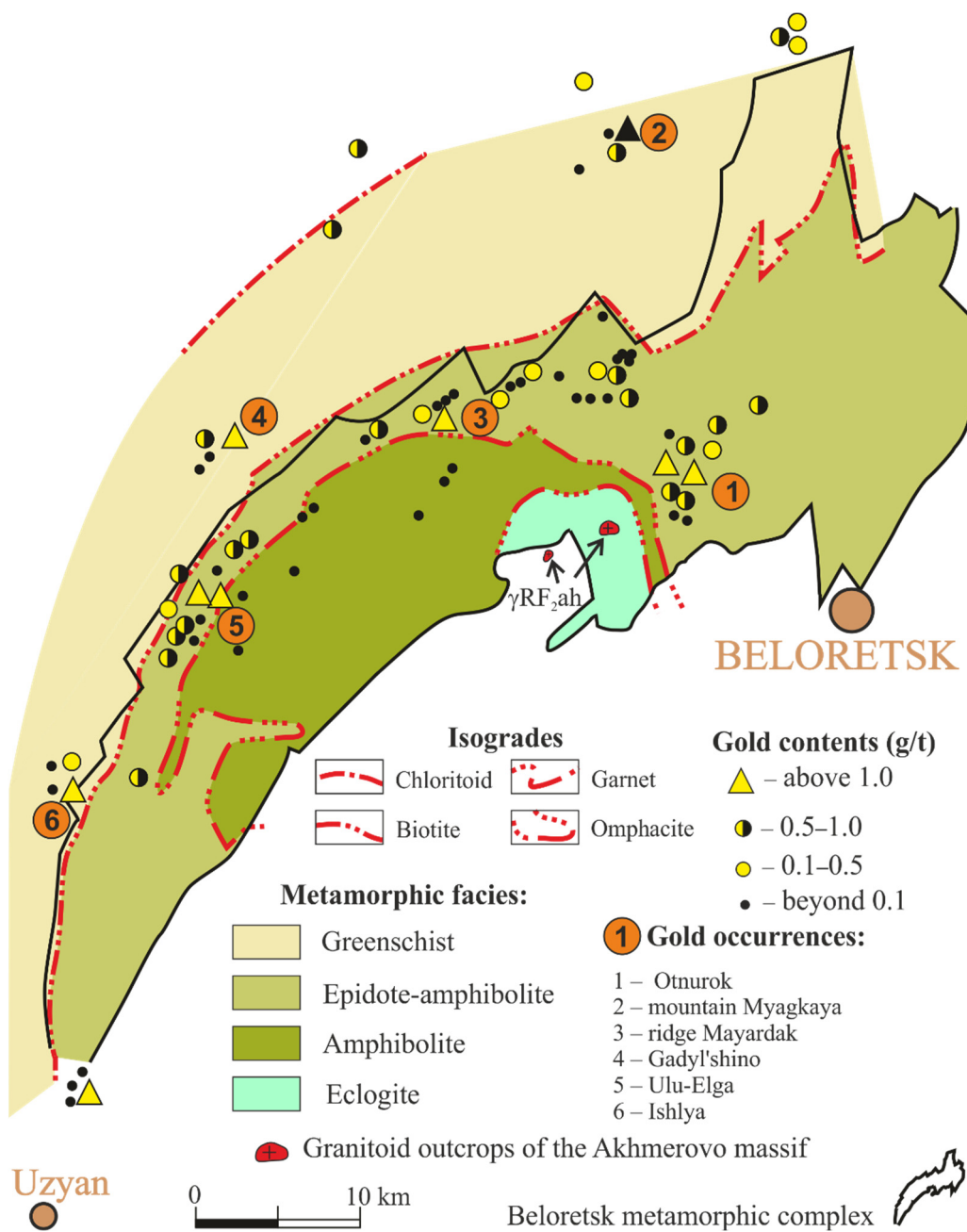


**Figure 5.** Scheme of the distribution of gold occurrences within the Beloretsk metamorphic complex (number of gold occurrences in Otnurok; also see Figure 1 (No. 1)) (from A.A. Alekseev et al. [76], simplified by the authors).

### 3.2. Zilair Megasyntorium

The problem of dating the age boundaries of metamorphic strata of the conjunction zone of the northern part of the Zilair Megasyntorium and the Uraltau Megantictorium is still debatable and has not been solved yet. The section of carbonaceous shales exposed 6 km southeast of Beloretsk town along the Beloretsk–Magnitogorsk highway on the watershed of the Yatva and Ukshuk rivers was earlier conventionally attributed to the Uraltau Megaantictorium [89]. However, the results of recent geological and survey work show that it belongs to the Zilair Formation (D<sub>3</sub>-C<sub>1</sub>zl) of the Zilair Megasyntorium [75] (Figure 6).

The section under study with a thickness of more than 150 m is represented by the alternation of dark gray thin-plate carbonaceous and micaceous–carbonaceous shales. Four

zones of crush and schist formation of rocks of about 10 m in width were identified within the section. Black shales are crushed into isoclinal folds of the southeastern strike, with widely developed flattening, flexural bends of layers, and cleavage. Intense muscovitization and chloritization of rocks are observed along the fracture planes; thin quartz veins occur, and quartz is cavernous and limonitized. Zones of intensive crushing are most commonly healed by quartz veins and veinlets.

Sulfide mineralization is observed practically along the whole section, and the intensity of mineralization clearly increases in the fracture and crush zones (Figure 7). Shales often contain pyrite leaching voids, occasionally oxidized pyrite crystals, or zones of complete hydration, which are represented by limonite ochres. In places, densely disseminated and continuous lenticular pyrite individuals in the form of 3–4 cm thick “ore layers” occur among black shales.

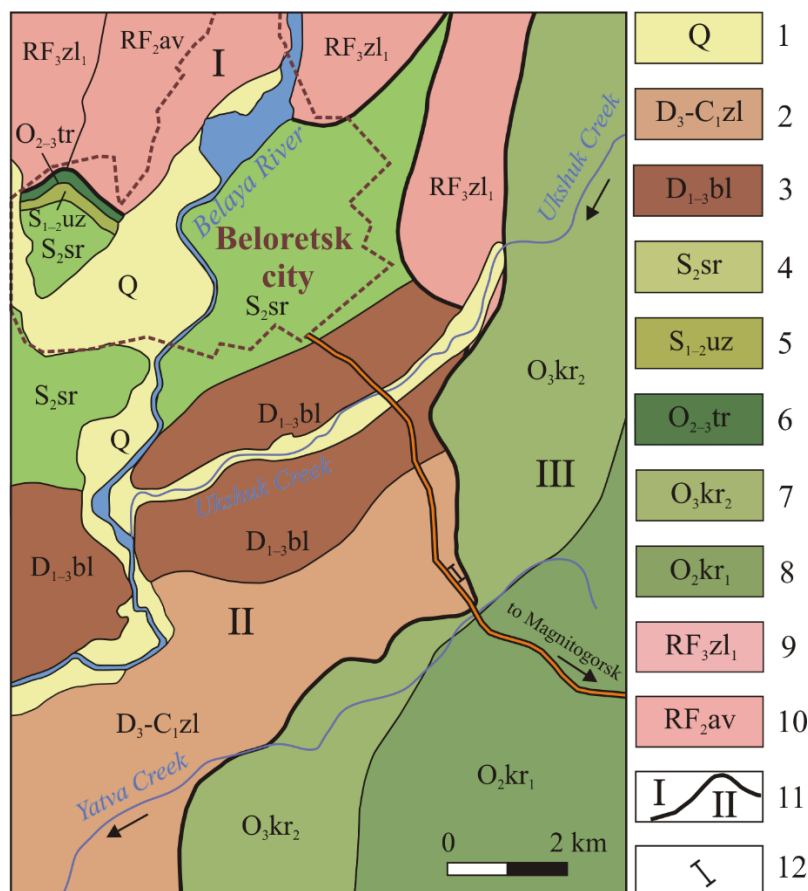


**Figure 6.** Geological map of the northern closure of the Zilair Megasyntlinorium (from Yu. G. Knyazev et al. [75], simplified by the authors). Legend: 1—Quaternary period (alluvial deposits), 2—Zilair Formation (sandstones, carbonaceous mudstones), 3—Bel Formation (limestones, sandstones), 4—Sermenevo Formation (dolomites, limestones), 5—Uzyan Formation (carbonaceous clay mudstones, siltstones), 6—Tirl'yan Formation (sandstones, siltstones), 7–8—Kurtash Formation: 7—upper sub-formation (quartzites, muscovite–chlorite–quartz shales), 8—lower sub-formation (aleuropsammite quartzites), 9—Zilmerdak Formation (micaceous quartzites), 10—Avzyan Formation (limestones, dolomites, carbonaceous–clay shales), 11—boundaries of structural formation zones: I—Bashkirian Megaanticlinorium, II—Zilair Megasyntlinorium, III—Uraltau Megaanticlinorium; 12—position of the cross-section under study (see Figure 7).

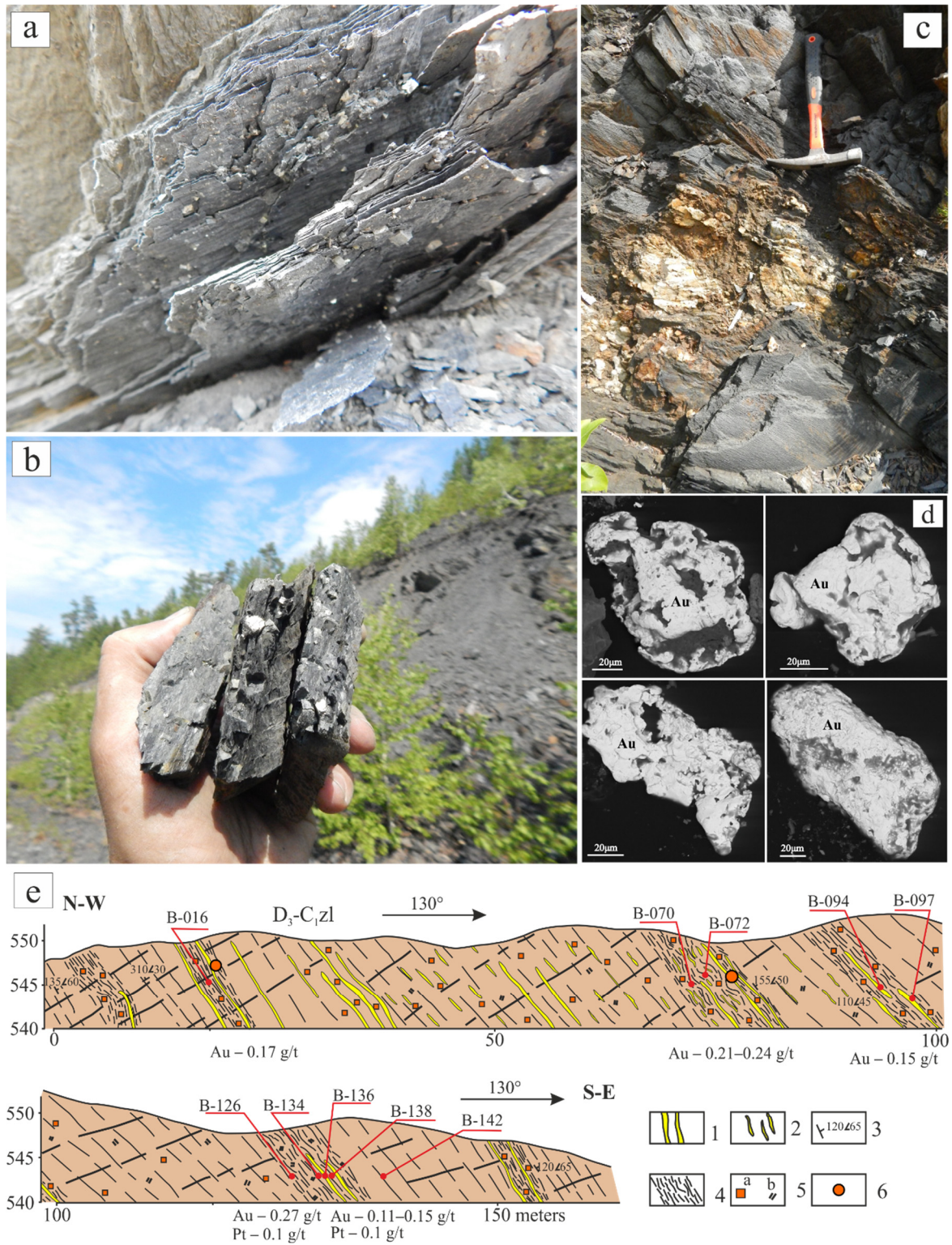


**Figure 7.** Sulfide mineralization (a,b), quartz veins (c), native gold from crushed samples of quartz veinlets and silicified black shales (d), and a cross-section (e) of the Zilair Formation along the Beloretsk–Magnitogorsk highway (see Figure 6 for the cross-section position). Legend: 1—quartz veins, 2—quartz veinlets, 3—layering and its occurrence elements, 4—zones of increased fracturing, 5—pyrite dissemination (a), silicified black shales (b), 6—sampling point (see Table 3).

**Table 3.** Contents of noble elements in the black shales of the Zilair Formation (g/t).

No.	Sample	Au	Ag	Pt	Pd
1	B-016	0.17	1.30	0.01	-
2	B-070	0.21	1.34	-	0.005
3	B-072	0.24	0.90	-	0.003
4	B-094	0.15	1.50	0.02	0.010
5	B-097	0.07	0.66	0.02	0.010
6	B-126	0.27	0.92	0.10	0.008
7	B-134	0.11	1.18	0.09	0.010
8	B-136	0.06	0.40	0.10	-
9	B-138	0.08	1.10	0.02	0.005
10	B-142	0.15	0.90	0.03	0.050

Note: The analysis was carried out at IGEM RAS (Moscow). Dash—content of the element is below the sensitivity threshold of the analysis.

We analyzed 10 samples of pyritized carbonaceous shale and limonitized vein quartz (Table 3). The most interesting results were obtained for Au—0.060–0.270 g/t (average 0.160 g/t). All Au contents are markedly higher than the ore anomaly (0.050 g/t). In addition to gold, the samples contain Pt—0.020–0.100 g/t (average 0.042 g/t) and Pd—0.005–0.050 g/t (0.011 g/t); other platinum group elements are present in amounts below the detection limit.

Black shales of the Zilair Formation, located at the intersection of large long-lived discontinuities that controlled the migration, redistribution, and mobilization of ore material, are of interest for further sampling works in this zone. Moreso, a band of carbonaceous deposits is traced in the northeastern direction towards Uraltau station.

### 3.3. Uraltau Meganticlinorium

The Uraltau zone, located between the Main Ural Fault in the east, the Zilair Megasynclinorium, and the Bashkir Meganticlinorium in the west, can be traced in the meridional direction from the latitude of the village of Kiryabinskoye to the Mugodzars (Figure 1). Until recently, this zone was identified on all geologic maps as a pre-Paleozoic (Riphean–Vendian) asymmetric anticlinorium structure with gentle western and steep eastern flanks. Currently, due to new findings of fauna, there has been a tendency to reconsider the stratigraphy and structure of this region. The Uraltau zone is interpreted as Early–Middle Paleozoic.

The area under study, known as the Novousmanovo area (Figure 8e), is located in the basin of the Beterya and Tupargass rivers. Tectonically, it is confined to the conjunction zone of the submeridional West Uraltau and latitudinal Burzyansk faults and is predominantly composed of the Ordovician phyllite-like shales, quartzite sandstones (Akbik and Belekey Formations), and Silurian–Devonian siliceous, siliceous–clay, carbonaceous–clay shales, and quartzite sandstones (Tupargass, Novousmanovo, and Ibragimovo Formations) [75]. A characteristic feature of these carbonaceous sediments is their high dislocation, i.e., the presence of zones of increased fracturing and anticlinal fold structures, which complicate the synclinal trough. In such zones, black shales are saturated with numerous quartz veins, metamorphosed, and contain sulfide mineralization. Sulfides are represented mainly by pyrite, chalcopyrite, chalcocine, pyrrhotite, and sphalerite and form rather thick zones (up to 10–25 m).

We analyzed metasomatically altered black shales, quartz, and feldspar–quartz veins and veins forming meridianally oriented zones in terrigenous rocks hundreds of meters wide and a few kilometers long for noble metals (Table 4). It is noteworthy that almost all types of veins contain varying amounts of ochreous iron hydroxides that fill numerous leaching voids. It is in the samples with iron hydroxides that platinoid concentrations of up to 2.0 g/t were obtained, among which Pd (up to 1.8 g/t) was predominant. Out of eighteen analyses for platinum group metals, six contained more than 1.0 g/t Pd, averaging 0.65 g/t. The highest Pt content was 0.36 g/t, averaging 0.12 g/t. The contents of other elements (Rh, Ru, Os, Ir) were no more than hundredths of g/t.

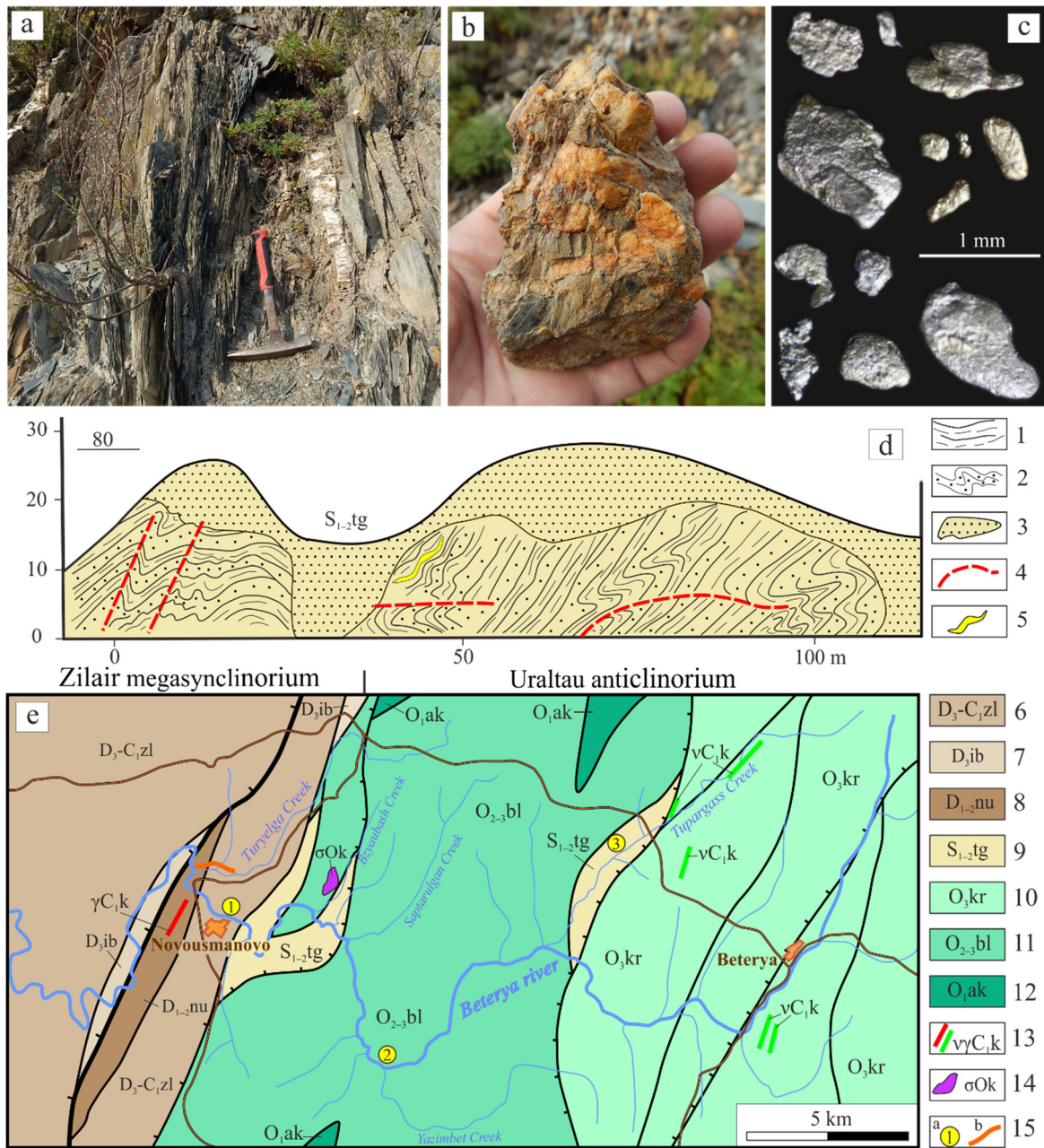


**Figure 8.** Quartz veins (a) and silicified black shales (b) of Zilair Formation (No. 1), native gold from the alluvium of Turyelga creek [90] (c), typical cross-section of Tupargas Formation (d) (No. 3), and geological scheme of the Novousmanovo ore area (e) (from Knyazev et al. [75], simplified by the authors). Legend: 1—black shales, 2—sandstones, 3—areas covered by soil, 4—faults, 5—quartz veins, 6—Zilair Formation (sandstones, carbonaceous mudstones), 7—Ibragimovo Formation (clay shales, siltstones), 8—Novousmanovo Formation (quartz sandstones and siltstones), 9—Tupargas Formation (carbonaceous shales), 10—Kurtash Formation (quartzites, muscovite–chlorite–quartz shales), 11—Belekei Formation (quartz sandstones and siltstones), 12—Akbiik Formation (sandstones), 13—Kananikol gabbro–granite complex, 14—Krakinskiy dunite–hartzburgite–gabbro complex, 15—position of black shale cross-sections (a), gold placer (b).

**Table 4.** Contents of noble elements in silicified and ferruginated carbonaceous shales of the Novos-manovo area (g/t) [59].

No.	Sample	Au	Ag	Pt	Pd	Rh	Ru	Os	Ir
1	Nu-112	0.04	0.99	0.23	0.08	0.01	0.02	-	0.02
2	Nu-114	0.01	0.86	0.05	1.40	-	0.04	-	0.01
3	Nu-115	-	1.30	0.01	0.71	0.01	0.04	0.03	0.01
4	Nu-117	-	0.72	0.01	0.12	0.01	0.05	-	-
5	Nu-118	-	1.20	0.10	1.80	-	0.06	0.03	-
6	Nu-126	-	1.40	-	0.11	0.02	0.08	-	0.01
7	Nu-132	0.23	1.10	0.36	-	-	-	-	-
8	Nu-135/1	0.07	2.90	0.15	0.47	-	0.01	0.06	0.01
9	Nu-353	0.03	1.30	-	0.31	-	0.01	-	-
10	Nu-355	-	2.10	0.08	0.63	0.01	0.01	-	-
11	Nu-356	0.04	0.70	0.02	0.25	-	0.01	-	-
12	Nu-357/1	-	0.34	0.07	1.30	0.01	-	-	-
13	Nu-357/2	-	0.20	-	-	-	-	0.04	-
14	Nu-359/1	-	1.70	-	1.80	0.03	0.02	-	-
15	Nu-360	-	1.50	-	0.95	0.01	-	0.04	-
16	Nu-362	-	1.20	-	0.57	-	0.02	-	-
17	Nu-363	0.19	1.30	-	0.07	0.08	0.05	0.04	-
18	Nu-364	0.04	3.20	-	0.68	0.01	-	-	0.02
19	Nu-2/3	0.59	3.10	0.02	0.01	-	-	-	-
20	Nu-2/5	0.28	1.70	-	0.03	-	-	-	-
21	Nu-2/7	0.5	2.50	-	-	-	-	-	-

Note: The analysis of Au and Ag was carried out at FGUP TSNIGRI (Moscow), PGE—IGEM RAS (Moscow). Dash—content of the element is below the sensitivity threshold of the analysis.

Gold contents in sulfidized carbonaceous shales, according to pit sampling data, range from 0.28 to 0.59 g/t, with silver concentrations of 1.7–3.1 g/t. These contents are within the range of ore concentrations of the halo zone, which commonly frames gold-bearing bodies. In this regard, such objects provide the potential for discovering primary industrial deposits among them. Pit sampling of quartz veins showed their low gold content. Most of the samples contain gold in the amount from 0.01 to 0.08 g/t and silver from 0.2 to 3.3 g/t. Only in some quartz veins do gold concentrations increase up to 0.23 g/t (Saptarulgan creek), 0.19 g/t (Turyelga creek), and 0.12 g/t (Bzaubash creek, Beterya River). Heavy concentrate sampling along these watercourses showed the presence of gold in the fluvial alluvium. The largest amount of the latter was found in the Bolshaya Turyelga creek draining quartz veins associated with terrigenous shale strata of the Betrya Formation and sandy shale deposits of the Zilair Formation. At the mouth of the creek for several hundred meters, commercial concentrations of schlich gold in the range of 0.6–2.3 g/m<sup>3</sup> are identified [90].

The results of sample analysis for W and Mo of vein quartz, quartz siltstones with iron hydroxides, and hematitized black shales showed the maximum value for W to be 0.019% and Mo to be 0.010%, which are, respectively, 190 and 100 times higher than the background contents [91]. Preliminarily, this ore mineralization can be associated with the intrusion of acidic composition at depth, the apophyses of which were found in the immediate vicinity of the top of Mt. Artlysh.

### 3.4. Main Ural Fault Zone

The territory under study is located in the northern part of the western flank of the Magnitogorsk Megasyntorium. Its complex geological and tectonic structure is due to its location opposite the Ufa ledge in the most compressed part of the Ural structures, where the structural material complexes formed in different periods and different geodynamic settings underwent fundamental changes during the collisional stages of the development of this territory, with the formation of thrust dislocations and paragenesis of shift and fault shift dislocations [61,92,93]. Carbonaceous shales are represented by narrow elongated blocks of the Ordovician age, spatially associated with ultrabasic rocks and the gabbro of

the melanocratic basement, and products of oceanic-type volcanism, representing a single Early Paleozoic ophiolite association.

The Siratur ore field is located in the northern part of the South Urals segment of the Main Ural Fault. Three primary gold deposits (Siratur, Kuzma–Demyanovskoye, and Kamyshakskoye) [94] and several gold occurrences (Badger Log, Bugor, Golenkiye Gorki, Razdolnoye) are known within its boundaries [95]. All of them are associated with the marginal eastern part of the submeridional band of carbonaceous, carbonaceous–chlorite–quartz, and chlorite–quartz shales of the Polyakovka Formation, reliably dated as the Ordovician by conodonts [96], as well as to the zone of its tectonic joint with serpentinites and ultrabasic rocks of the Nurali Massif, the age of which, according to the latest data, is  $450 \pm 4$  Ma [97–99] (Figure 9).

Carbonaceous shales belong to the low-carbonaceous type and fall into the fields of terrigenous–carbonaceous and carbonate–carbonaceous formations, which together with the presence of carbonates in the section, suggests that they were formed in the shallow and the coastal shallow water region of the sedimentary basin. The terrigenous material in the process of sedimentation of these deposits underwent minimal transport and takes its origin from the rocks of predominantly basic and medium composition [100]. Carbonaceous matter represented by vein-like and flake-like particles is of biogenic nature, and it underwent metamorphism under the conditions of high-temperature subfacies of greenschist facies.

Geological exploration, geochemical, mineralogical, and petrological studies carried out on the territory under study revealed that gold mineralization in black shale deposits is represented mainly by the gold–sulfide streaky disseminated type, and in the listvenite–beresite complex, by the gold–quartz low-sulfide vein streaky type [94]. The Siratur deposit includes Feldsher (in the north), Central Siratur (in the center), and South Siratur (in the south) gold ore areas and stretches for 3.7 km with a width of 100 to 400 m. There are four ore bodies within its boundaries, the first of which (eastern) is the main body traced for a distance of 2.1 km, with the following average parameters: the thickness is 3.0 m and the gold content is 2.12 g/t (Table 5). This ore body is confined to the lying contact between the black shale series with listvenites and has a steep ( $85^\circ$ ) western dip. Sulfide mineralization in the rocks of the ore zone occupies up to 10% and is represented by pyrite, chalcopyrite, and arsenopyrite. Pyrrhotite and sphalerite are also found in carbonaceous shales. Three other ore bodies are located among the black shales parallel to the first body; they are not contoured in strike and dip. There is a clear regularity within the ore zone—the highest gold content is detected in the areas with streaky vein (“reticulate”) silicification and a high degree of sulfidization, especially in the zone of quartz–albite rocks. In addition to the above-mentioned ore bodies, the so-called Shirotnaya vein was also observed in the extreme southern part of the Siratur deposit. It is confined to the borders of the fracture zone feathering the Main Ural Fault. The ores are bounded by the zone of the crush of carbonaceous shales and are composed of the quartz low-sulfide vein streaky type. Gold distribution in them is uneven. In the areas densely penetrated by quartz veins, its content reaches 25 g/t.

Within the Siratur deposit and Golenkiye Gorki and Feldsher occurrences, we obtained several dozens of gold particles in the process of washing the gruss–rubble weathering crusts developed on carbonaceous shales and listvenites.

Microprobe analysis allowed us to divide gold pits into two groups, the first of which (the main ore body and Shirotnaya vein of the Siratur deposit, Feldsher occurrence) is characterized by high fineness (900–980) (Figure 9(b2)), and the second (gold–sulfide ores of Siratur deposit and Golenkiye Gorki occurrence) contains a considerable amount of silver (up to electrum) (67%–82% Au, 17%–33% Ag, and up to 0.36% Cu). When studying the polished sections of gold–sulfide ores from the Siratur deposit, low fineness gold was also found in pyrite—Au = 50%–55%, Ag = 45%–50% (Figure 9(b3)).

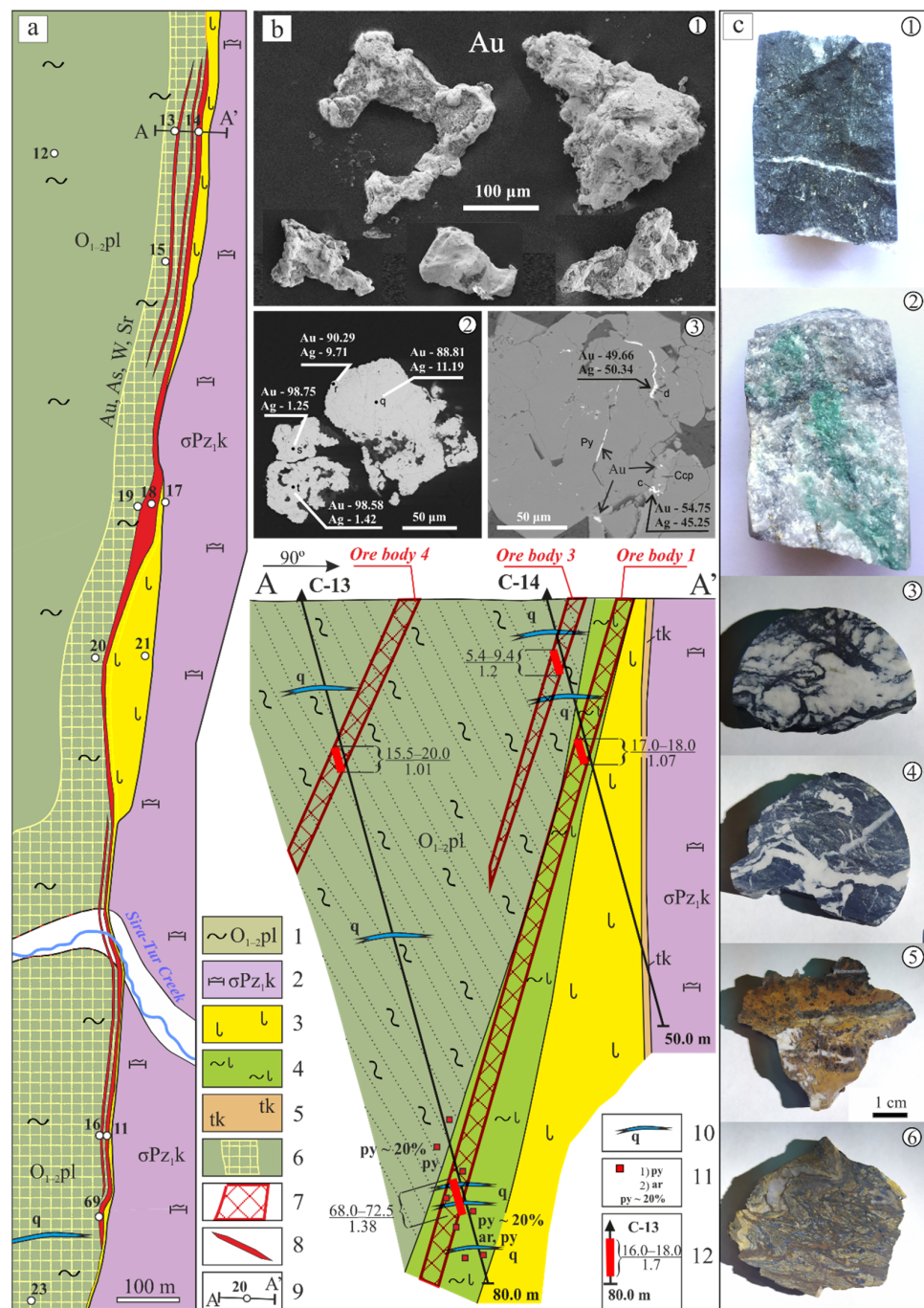


**Figure 9.** Geological map and cross-section (a) [94], electron microscope images of native gold from weathering crusts (b1), high fineness gold from quartz veins (b2), low fineness gold in pyrite from carbonaceous shale (b3), gold-sulfide ores (c1), listvenites (c2), and silicified black shales (c3–6) of the Siratur ore field (c). Legend: 1—Quaternary system (alluvial deposits), 2—Polyakovka Formation (sericite-chlorite-quartz, carbonaceous-chlorite-quartz schists), 3—Kempirsai-Voikar gabbro-hyperbasite complex (Nurali massif), 4—listvenites on carbonaceous schists and ultrabasic rocks, 5—talc-carbonate rocks, 6—zone of tectonic reworking of carbonaceous shales with intensive sulfidization, to which the complex geochemical anomaly Au, As, W, and Sr is confined. Ore body: 7—in a cross-section, 8—on the plan; 9—wells and cross-sections A-A', 10—quartz veins and veinlets, 11—sulfide mineralization and its percentage to the total mass of the rock: (1) pyrite; (2) arsenopyrite. 12—wells in a cross-section and their depth, number, and testing results (numerator is the interval, m; denominator is the average Au content, g/t).

**Table 5.** Contents of Au and Ag in black shales and listvenites of the Siratur deposits (g/t).

No.	Sample	Au	Ag	No.	Wells	Depth (m)		Au
1	GG-2.1	0.25	0.14	26	W-69	1.0	2.0	0.56
2	GG-2.3	0.35	0.71	27	W-69	2.0	3.0	0.88
3	GG-2.5	0.23	0.90	28	W-69	3.0	6.0	0.83
4	GG-2.7	0.28	0.09	29	W-69	11.0	13.0	0.42
5	GG-2.8	0.25	0.27	30	W-69	16.0	18.0	1.70
6	GG-4.1	2.03	0.95	31	W-19	128.3	130.4	1.21
7	GG-5.3	0.43	0.03	32	W-19	130.4	131.4	0.62
8	Kam-1.1	0.73	0.31	33	W-19	131.4	133.4	14.91
9	St-1	0.19	0.46	34	W-19	135.9	138.0	0.54
10	St-15-73	0.35	0.03	35	W-14	5.4	6.4	1.15
11	St-23-34	0.31	0.05	36	W-14	6.4	7.4	1.33
12	St-28-66	0.38	0.06	37	W-14	7.4	8.4	0.75
13	St-28-70	0.32	0.33	38	W-14	8.4	9.4	0.81
14	St-33-22	0.00	0.68	39	W-14	17.0	18.0	1.07
15	St-5	0.2	0.28	40	W-13	4.0	6.0	1.13
16	St-53-33	0.40	10.5	41	W-13	7.2	9.7	0.52
17	St-6	0.49	0.18	42	W-13	12.0	13.5	0.48
18	St-Sht/3	0.23	0.52	43	W-13	13.5	15.5	0.51
19	F-4	0.24	0.54	44	W-13	15.5	17.4	1.44
20	F-4.4	0.23	0.02	45	W-13	17.4	18.9	1.07
21	F-4.8	0.32	0.24	46	W-13	18.9	20.9	1.26
22	F-4.9	0.26	0.13	47	W-13	20.9	21.4	0.76
23	F-5	0.24	0.24	48	W-13	25.4	26.9	0.49
24	Fk-8.12	0.31	0.09	49	W-13	68.0	71.0	0.80
25	Fk-8.14	0.44	0.06	50	W-13	71.0	72.5	2.73

Note: 1–25—authors' data (the analyses were carried out at the Institute of Geology UFRC RAS (Ufa) using the atomic absorption method), 26–50—data of JSC «Bashkirgeologiya» (using the atomic absorption method).

Thus, the carbonaceous sediments contained an increased concentration of gold. As a result of the subsequent long history of the development of the Magnitogorsk Megazone in the early and middle Paleozoic (oceanic and island-arc stages), the black shale strata underwent intense submersion, catagenetic transformations, and zonal near-fault metamorphism in the conditions of greenschist and epidote–amphibolite facies. At that time, streaky disseminated gold–sulfide ores (fineness 670–820) were formed. During the collisional stage of development of the Southern Urals ( $C_2-P_1$ ), most likely due to the hydrothermal activity of the granitoids of the Balbuk complex, vein streaky disseminated gold–quartz low-sulfide ores were formed. These contain high fineness (940–970) gold and occur in the rocks that underwent sodium metasomatism. Numerous differences in both types of ores result from the conditions of formation of mineralization and, probably, from the composition of fluid systems, the evolution of which led to their formation. On the whole, the Siratur deposit can be attributed to the polygenetic and polychronic types. It is, so far, the only object in the South Urals, which is located in black shale deposits of the ophiolite association and is of great interest for further prospecting and exploration works.

The Chernoe Ozero occurrence includes the following. The deposit is located 2.0 km east of the town of Karabash, where it is confined to borders the area of development of black shale terrigenous deposits of the Polyakovka Formation ( $O_{1-2pl}$ ) (Figure 10) [101].

They are represented by interbedded tuffs, tuffites, various shales, sandstones, conglomerates, and talc-rich rocks. Among them, there are layers of carbonaceous–clayey, carbonaceous–siliceous, and carbonaceous–sericite–quartz shales. Terrigenous sediments are traced in a submeridional direction along the eastern slope of the Karabash Mountains in the form of a short (less than 1 km) band of over 3.5 km.

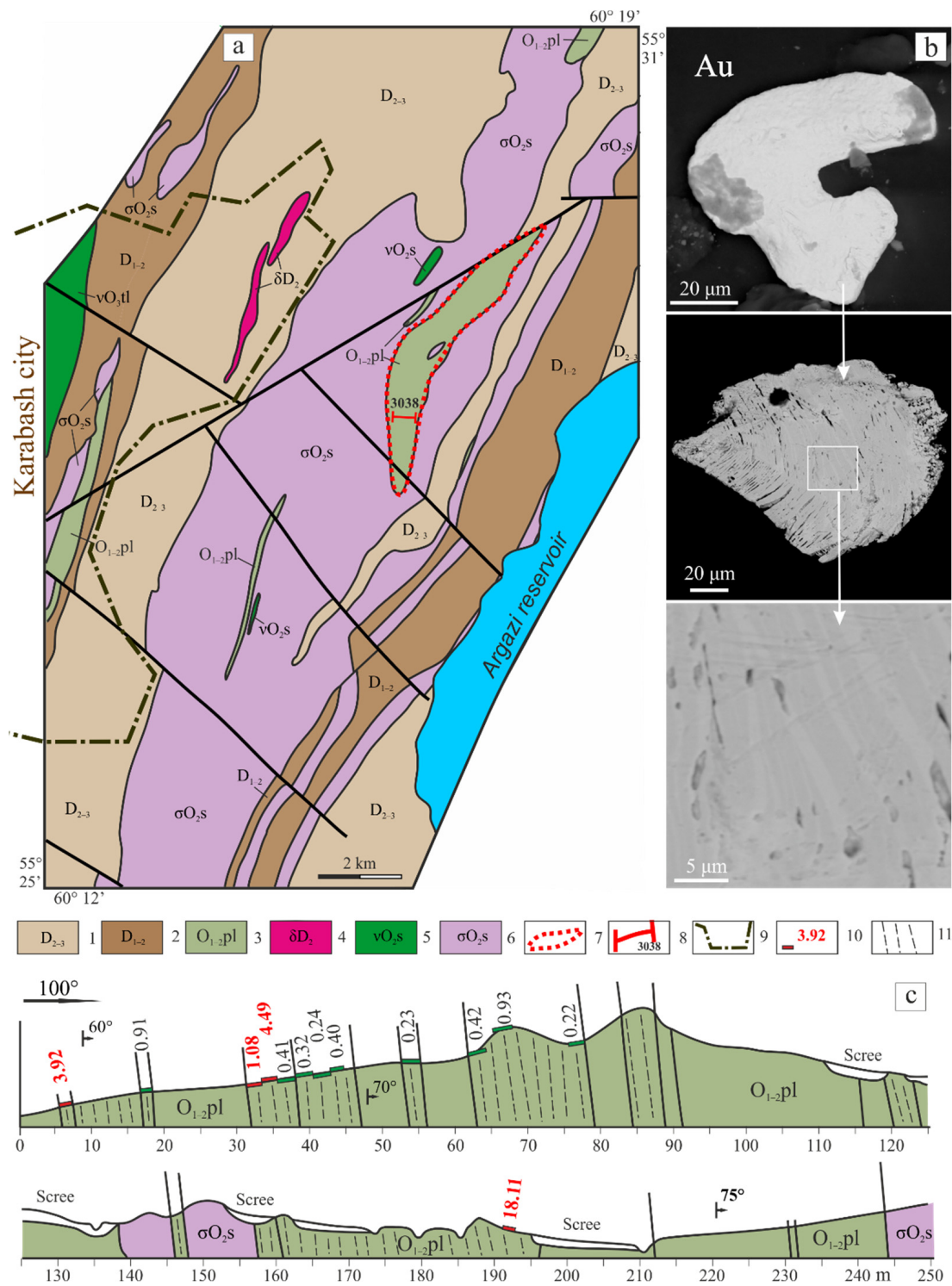


**Figure 10.** Scheme of the geologic structure of the Karabash massif (a), geologic cross-section of the Polyakovka Formation with the results of trench sampling at the Chernoe Ozero gold ore field (c) [101], and native gold from carbonaceous shales with a characteristic exsolution structure Au-Cu (b). Legend: 1—Karamalytash and Ulutau Formations; 2—Irendyk Formation; 3—Polyakovka Formation; 4—Salavat diorite–plagiogranite complex; 5, 6—Sakmarian complex (5—gabbro, 6—harzburgites, dunites, serpentinites); 7—complex geochemical anomaly; 8—location of the cross-section; 9—border of the city of Karabash; 10—intervals of trench sampling and gold content in g/t: red—more than 1 g/t and green—0.2–1 g/t; 11—carbonaceous shales.

As a result of 1:200,000 scale geological and survey works, the staff of OJSC “Chelyabinskgeosyemka” established that terrigenous sediments have elevated contents of copper, zinc, lead, silver, and arsenic (in some samples—cadmium, antimony, and bismuth). Using the data from previous works, an extensive geochemical anomaly of these elements, covering most of the terrigenous sediment distribution area, was identified. It was pointed out that higher concentrations of some anomaly-forming elements were found in the layers with high organic carbon content. Owing to this, in the well-exposed part of the area (outcrop 3038), trenching sampling of black shale sediments was carried out, with the length of samples being 1.5 to 2.5 m (Figure 10c). It was found that all 23 samples contained gold, with concentrations ranging from 0.019 to 18.11 g/t (averaging 1.47 g/t) (Table 6).

**Table 6.** Results of the sampling of carbonaceous rocks of the Chernoe Ozero occurrence (g/t) [59].

No.	Sample	Au	Pd	Pt	Rh	Ir
1	3038/6–7.5	3.92	0.008	0.002	0.001	0.007
2	3038/17–19	0.91	0.021	0.002	0.001	–
3	3038/32–34	1.08	0.061	0.001	0.004	0.003
4	3038/34–36.2	4.91	0.036	0.001	0.002	–
5	3038/36.2–38.4	0.41	0.020	0.001	0.004	0.004
6	3038/38.6–40	0.32	0.041	0.002	0.006	0.001
7	3038/40.8–43	0.24	0.012	0.002	0.004	–
8	3038/43–45	0.40	0.008	–	0.004	0.003
9	3038/45–47	0.05	0.016	0.001	0.003	0.009
10	3038/53.5–56	0.23	0.016	0.003	0.004	0.004
11	3038/63–65	0.48	0.033	0.002	0.007	0.004
12	3038/65–67	0.16	0.011	–	0.002	–
13	3038/67–69	0.93	0.050	0.002	0.003	–
14	3038/69–71	0.07	0.014	0.018	0.001	0.002
15	3038/71–73	0.12	0.001	0.001	0.001	–
16	3038/73–75	0.02	0.018	0.002	0.001	–
17	3038/75–77	0.08	0.082	0.001	0.001	–
18	3038/77–79	0.22	0.055	0.002	0.079	0.010
19	3038/84.5–86.7	0.09	0.010	0.014	0.002	0.001
20	3038/86.7–89	0.70	0.140	–	0.001	–
21	3038/160–162	0.12	0.060	0.004	0.001	0.003
22	3038/188	0.13	0.018	0.002	0.002	0.009
23	3038/191–193	18.110	0.026	–	0.003	0.004

Note: Dash—content of the element is below the sensitivity threshold of the analysis. The analysis was carried out at IGEM RAS (Moscow).

It is noteworthy that the highest gold contents were detected in the intensely dislocated and sulfidized zones of carbonaceous metasilstones and meta-sandstones. In addition, the samples contain platinum group elements: palladium—from 0.0005 to 0.14 g/t; platinum—from <0.0005 to 0.018 g/t; rhodium—from 0.0009 to 0.079 g/t; and iridium—from <0.0005 to 0.010 g/t. We washed out several small high fineness gold grains from carbonaceous shales (Figure 10b). They are marked by the Au-Cu exsolution structure, which is characteristic of gold from the Zolotaya Gora deposit in the Karabash ultramafic massif [102,103].

Thus, the presence of elevated gold contents in carbonaceous sediments of the Chernoe Ozero occurrence, characterized by the abnormal concentrations of indicator elements (Cu, Zn, Pb, Ag, As, Sb, Cd, Bi), suggests their high prospects for the discovery of commercial gold mineralization associated with the black shale formation. This object deserves further study and special prospecting works.

### 3.5. Magnitogorsk Megasyntorium

The Amur stratiform zinc deposit is located in the easternmost part of the Magnitogorsk Megasyntorium, 1.0–1.5 km west of the large Suunduk granite massif, and it is confined to the borders of the western limb of the meridionally elongated brachyanticlinal

fold (Figure 11). According to the geological exploration and prospecting works of the past years, its structure includes volcanogenic ( $D_{2-3am}$ ) and terrigenous-carbonate ( $D_{2am}$ ) substrata of the Amur Formation and the Rymnik Formation ( $O_{1rm}$ ). Intrusive complexes are represented by gabbro-dolerites of the Cherkashi complex ( $vC_1$ ) and granites of the Suunduk massif ( $\gamma C_1-P_1$ ) [104,105] (Figure 11).

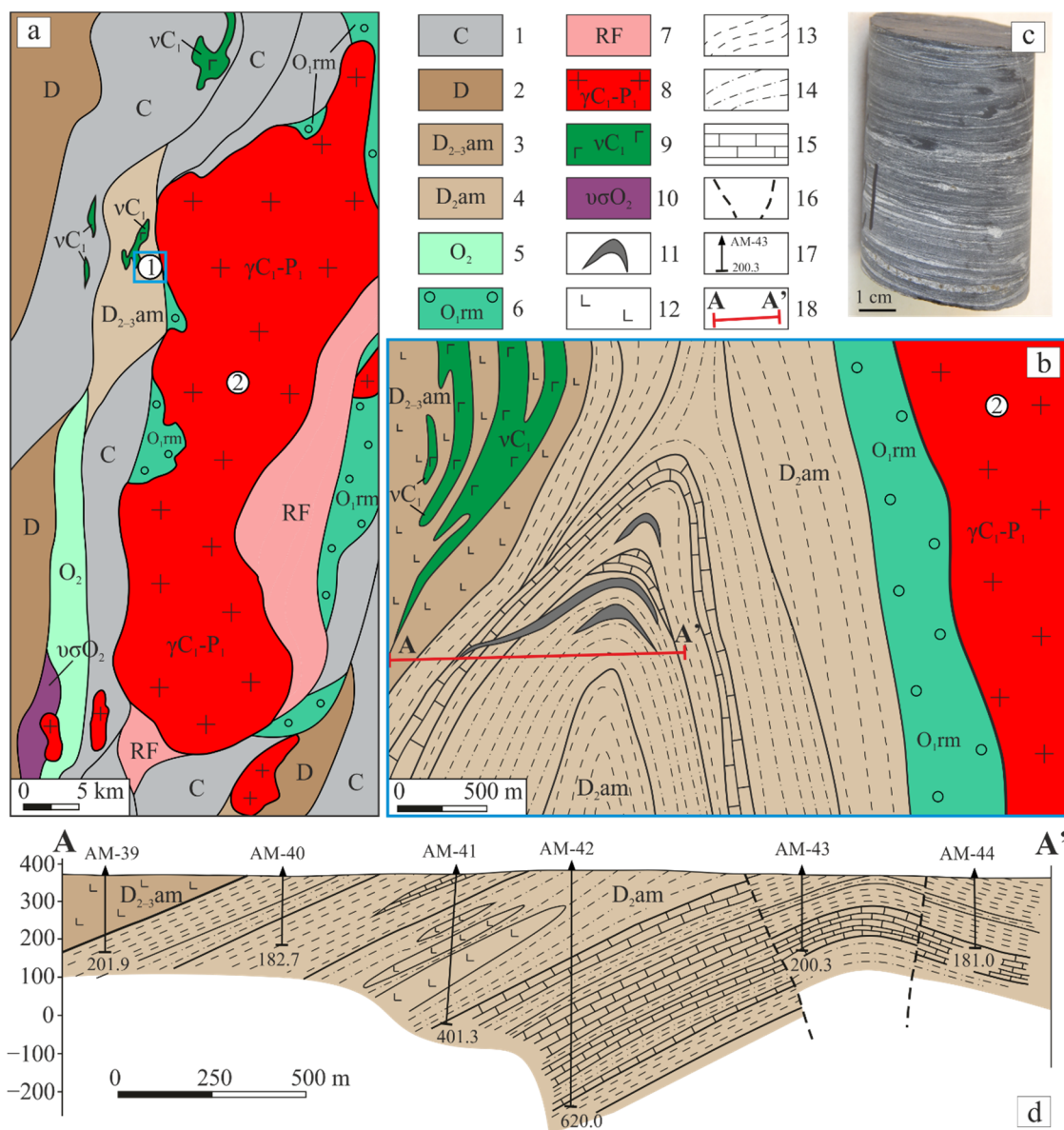


**Figure 11.** Geological map of the framing of the Suunduk massif (a), geological map (b), carbonaceous shale (c), and a cross-section (d) of the Amur deposit. Compiled on the basis of materials [75,106,107]. Legend: 1—carboniferous undissected complexes (sandstones, limestones, basalts), 2—Devonian undissected complexes (basalts and their tuffs), 3—volcanogenic substrata of the Amur Formation (basalts and their tuffs), 4—terrigenous-sedimentary substrata of the Amur Formation (carbonaceous shales, limestones, basalts), 5—Novoorenburg Formation (shales, sandstones), 6—Rymnik Formation (sandstones, gravelites, conglomerates), 7—undissected Riphean metamorphic complexes, 8—granites, leucogranites, and granodiorites of the Suunduk massif, 9—gabbro-dolerites of the Cherkashi complex, 10—ultrabasic rocks of the Kulikov complex, 11—brown ironstones, 12—basalts, 13—terrigenous-carbonaceous shales, 14—carbonate-carbonaceous shales, 15—limestones. Figures in circles: 1—Amur deposit, 2—Suunduk granite massif; 16—faults; 17—wells in a cross-section; 18—location of the cross-section A-A' (d).

Formations of the volcanogenic sequence (D<sub>2-3am</sub>) are developed in the western part of the deposit area. They are represented mainly by tuffs, tuffites, and subalkaline high-titanic basalts, penetrated by dikes and sills of gabbro and gabbro–dolerites (vC<sub>1</sub>).

The Amur stratiform zinc deposit (SEDEX type) occurs in the upper part of the terrigenous carbonate strata. The ore body containing massive and banded zinc–sulfur–coal ores occurs conformably with the general layering of rocks and has a submeridional strike, stratiform shape, and a gentle (15–30°) westerly dip with monoclinical bends [108]. The sulfide ores are composed of ore-forming minerals, pyrite and sphalerite, and minor minerals, pyrrhotite, galena, and chalcopyrite. Arsenopyrite, jordanite, boulangerite, silver-bearing tennantite, lead-bearing gray ore (up to 7.9 wt.% Ag), cobalt sulfoarsenides, grinokite, ulmannite, and gold–mercury silver (Ag<sub>0.75</sub>Hg<sub>0.20</sub>Au<sub>0.05</sub>) myargyrite, xanthoconite, and stromeyerite are rare [109,110]. Brown ironstones spread on ores under near-surface conditions were found to contain high-grade gold in the form of grains up to 10 microns in size and rare grains of iodargyrite up to 3 microns in size [111].

Terrigenous–carbonate deposits (D<sub>2am</sub>) are developed in the central part of the structure and are represented by two beds. (1) The lower one is composed of rhythmically alternating siltstones, clayey, carbonaceous–clayey, and siliceous–clayey shales, and marbleized limestones; (2) the upper one consists mainly of carbonate–clayey–carbonaceous shales. The total thickness of the uncovered sediments is about 850 m. The problem of the age of the strata is still debatable. Owing to K.S. Ivanov’s identification of conodont in the carbonate rocks of the strata, the lower boundary of the age is not older than the Silurian [108]. The remains of crinoids were collected in plate carbonaceous–siliceous shales 3 km higher up the Amur settlement, which suggests their Silurian–Middle Devonian age [112]. The rocks were metamorphosed in the conditions of greenschist facies, with local occurrences of a higher-temperature stage of metamorphism in the eastern part of the deposit, which is the closest to the Suunduk massif [113]. At the contact of terrigenous black shale–carbonate sediments with overlying volcanogenic formations, there is a rather thick zone of crush and stratification, which is accompanied by the linear weathering crusts penetrating to depths of up to 250 m.

In the area under study, we carried out trench sampling of sulfidized and silicified carbonaceous shales for gold and platinum, the results of which are presented in Table 7.

**Table 7.** Contents of noble metals in the samples from the carbonaceous strata of the Amur deposit (g/t) [106].

No.	Sample	Au	Pd	Pt	Rh	Ir
1	AM-4/77	0.100	0.077	0.014	0.007	0.011
2	AM-9/187	1.650	0.280	0.004	0.007	0.003
3	AM-9/341	0.110	0.550	0.007	–	–
4	AM-15/139	0.053	0.220	0.002	0.001	0.004
5	AM-15/222	0.120	0.210	–	0.002	0.006
6	AM-17/154	0.017	0.001	–	–	–
7	AM-19/245	0.096	0.120	0.007	–	0.003
8	AM-22/371	0.011	0.004	0.003	–	–
9	AM-32/532	0.290	–	–	–	–
10	AM-32/545	0.028	0.004	0.004	–	–
11	AM-33/364	0.011	0.012	0.005	–	–
12	AM-33/610	0.013	0.003	–	–	–
13	AM-37/522	0.009	0.011	0.011	–	–
14	AM-38/490	0.042	0.028	0.062	–	–
15	AM-45/602	0.002	0.013	0.012	–	–
16	AM-46/468	0.009	0.034	0.060	–	–
17	AM-49/275	0.031	0.004	0.016	–	–
18	AM-50/593	3.190	0.150	0.015	0.002	–

Table 7. Cont.

No.	Sample	Au	Pd	Pt	Rh	Ir
19	AM-50/596	0.120	0.140	0.014	0.002	0.003
20	AM-55/517	0.061	0.120	0.009	0.003	0.006
21	AM-56/450	0.180	0.083	0.003	–	0.028
22	AM-58/217	0.350	0.330	0.520	0.039	0.019
23	AM-60/598	0.070	0.080	0.003	0.001	0.016
24	AM-62/500	0.025	0.098	0.007	0.002	0.023
25	AM-66/190	0.010	0.100	0.009	0.004	0.010
26	AM-67/121	0.270	0.650	0.005	0.003	0.016
27	AM-69/421	1.790	0.090	0.006	0.002	0.014
28	AM-69/589	0.022	0.160	0.009	0.006	0.036
29	AM-70/481	0.006	0.063	0.018	0.002	0.014
30	AM-71/432	–	0.020	0.011	0.003	0.005
31	AM-73/290	0.026	0.120	0.004	0.001	0.004
32	AM-74/209	0.053	0.290	0.014	0.007	0.005
33	AM-75/156	0.099	0.390	0.009	0.002	–
34	AM-76/494	0.091	0.061	0.007	0.016	0.006
35	AM-84A/374	0.040	0.120	0.003	0.014	0.011
36	AM-99/170	0.025	0.030	0.010	–	0.001
37	AM-102/180	0.190	0.072	0.003	–	0.009
38	AM-103/164	0.024	0.014	0.004	–	0.022
39	AM-105/247	0.021	0.079	0.015	–	0.008
40	AM-106/145	0.039	0.025	0.001	–	0.020

Note: Dash—content of the element is below the sensitivity threshold of the analysis. The analysis of Au was carried out at FGUP TSNIGRI (Moscow) and PGE at IGEM RAS (Moscow).

The average gold content of 75 samples in the rocks was 0.13 g/t, which corresponds to the level of ore anomaly. The maximum contents of gold in carbonaceous shales are 3.19, 1.79, and 1.65 g/t and are typical of either the eastern flank of the deposit or its northeastern section. In terms of platinum, the deposits under consideration are less interesting; their average content is five times lower than that of palladium and equals a few hundredths g/t. At the same time, one sample with a concentration of 0.55 g/t differs sharply from all the others, and it is also in the abnormally high concentrations of gold and palladium. For iridium and rhodium, all contents are either within the background or within detection limits (average Ir content is 0.010 g/t, Rh is 0.05 g/t). Sulfidized (pyrite, pyrrhotite) carbon-bearing rocks of the ore-bearing terrigenous strata are promising for palladium, the maximum concentrations of which are 0.65 and 0.55 g/t. It is noteworthy that all analyzed samples show a consistently high palladium content in the wells located in the easternmost part of the volcanogenic strata near its contact with the terrigenous strata. This is a good indicator for further analytical studies of carbonaceous formations.

### 3.6. Aramilsko–Sukhtelinsk Synclinorium

The Larino granite–gneiss dome is located at the boundary of the Magnitogorsk and Aramilsko–Sukhtelinsk Synclinorium and it is the southern continuation of the Ilmenogorsk–Sysert Uplift [64]. Stratigraphically, the following strata are distinguished in the area under consideration: Bulatovo (S<sub>1</sub>-D<sub>1</sub>bl) and Krasnokamensk (D<sub>3</sub>kr) Formations (Figure 12). Carbonaceous sediments are present and clearly predominate only in the composition of the former.

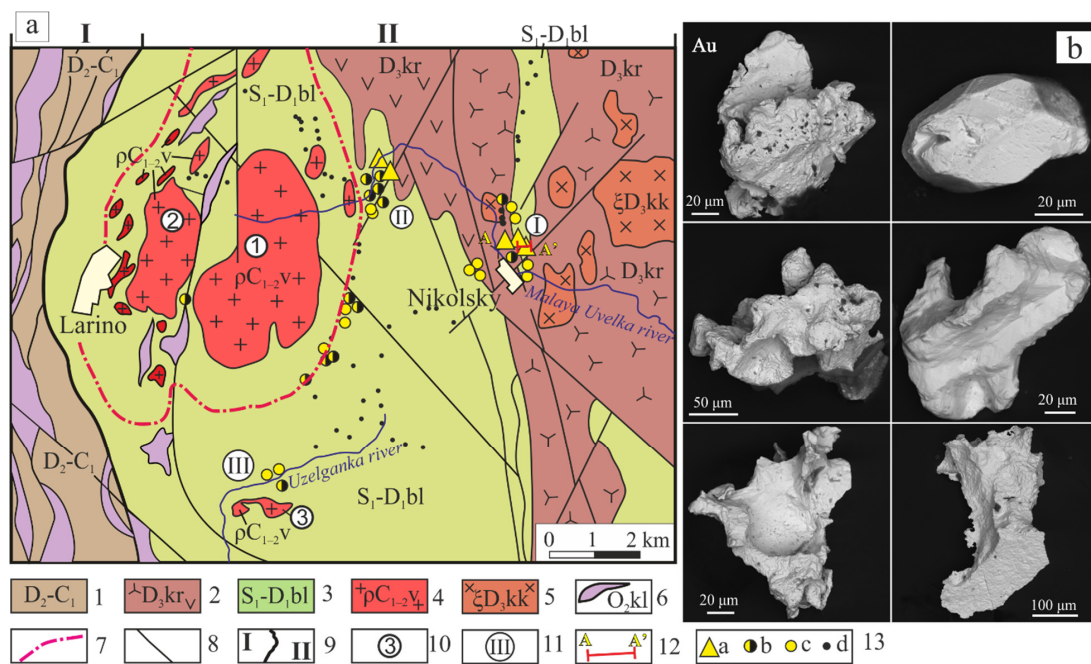


**Figure 12.** Geological structure of the Larino granite–gneiss dome (according to [114–116]) (a) and native gold from silicified and ferruginated black shales of the Bulatovo Formation (b). Legend: 1—volcanogenic–sedimentary complexes, undissected; 2—Krasnokamenka Formation (volcanomic sandstones and siltstones, acidic tuffs, trachybasalts and their tuffs); 3—Bulatovo Formation (carbonaceous shales and siltstones); 4—Varshav complex (muscovite granites with garnet, granitogneisses); 5—Krasnokamensk complex (syenites, quartz monzodiorites); 6—Kulikov complex (apodunite, apogartzburgite serpentinites); 7—boundary of amphibolite and epidote–amphibolite facies of metamorphism; 8—faults; 9—structure formation zones: I—Magnitogorsk Megasyntorium, II—Aramil–Sukhtelinsk zone; 10—names of massifs: 1—Pervomay, 2—Larino, 3—Pridannikovo; 11—gold occurrences—I—Nikolsky, II—Malouvelsk, III—Pridannikovo; 12—location of the cross-section A–A' (see Figure 13d); 13—samples with gold content (g/t): a—more than 1.0, b—0.5–1.0, c—0.1–0.5, d—less than 0.1.

The Bulatovo Formation has a fairly homogeneous composition. These are predominantly siliceous–carbonaceous shales, which in places alternate with clay–siliceous–carbonaceous varieties. Interlayers of basalts and tuff siltstones are observed in the lower parts of the section. The total thickness of the Bulatovo Formation is more than 900 m. Its age is based on graptolite fauna found near the village of Bulatovo, which allows us to date the strata as the Late Llandovery Wenlock. Near Mirny settlement, V.N. Puchkov and K.S. Ivanov [117] discovered conodonts characteristic of the Late Silurian and Devonian.

The immediate frame of the Larino and Pervomay massifs is composed of apovolcanic amphibolites, garnet–mica, garnet–amphibole plagioshales, graphitic quartzites, and siliceous–carbonaceous schists of the Bulatovo Formation. From granitoids to schists, a series of concentric high-gradient zones of metamorphism is observed. Mineral paragenesis of amphibolite facies at a distance of several kilometers is replaced by associations of epidote–amphibolite and greenschist facies. For the rocks of the epidote–amphibolite facies, the parameters of metamorphism are  $T = 530–550\text{ }^{\circ}\text{C}$  and  $P = 8.0–8.4\text{ kbar}$  [116]. Numerous veins of granular and milky-white quartz are associated with granites [118].

The most representative sections of the Bulatovo Formation were observed along the floor and sides of a gravel quarry near the northern outskirts of Nikolsky settlement and in a small pit on the right bank of the Malaya Uvelka river. Detailed geological mapping of the eastern frame of the Larino dome and sampling for noble metals of highly metamorphosed, sulfidized, and silicified carbonaceous sediments of the Bulatovo Formation showed high gold contents (Table 8), some of which are shown in Figure 12. The quarry near the dam in

the upper reaches of the Malaya Uvelka river, where gold contents of 3.6 and 4.9 g/t were detected, is worth special attention (Figure 13). Platinoid contents in carbonaceous shales of the Larino dome framing are low and equal to 0.05 g/t Pt and 0.1 g/t Pd (averaging 0.06 g/t for 20 samples).

We washed and analyzed small gold particles of  $0.05 \times 0.15$  mm in size (Figure 12b) in the samples from quartz veins developed among carbonaceous shales near the Nikolsky and Ushtaganka settlements. Gold particles are of high fineness (up to 918) and contain minor impurities of arsenic, selenium, and copper, which is typical of native gold at the majority of deposits of the Ural gold–quartz formation [4].

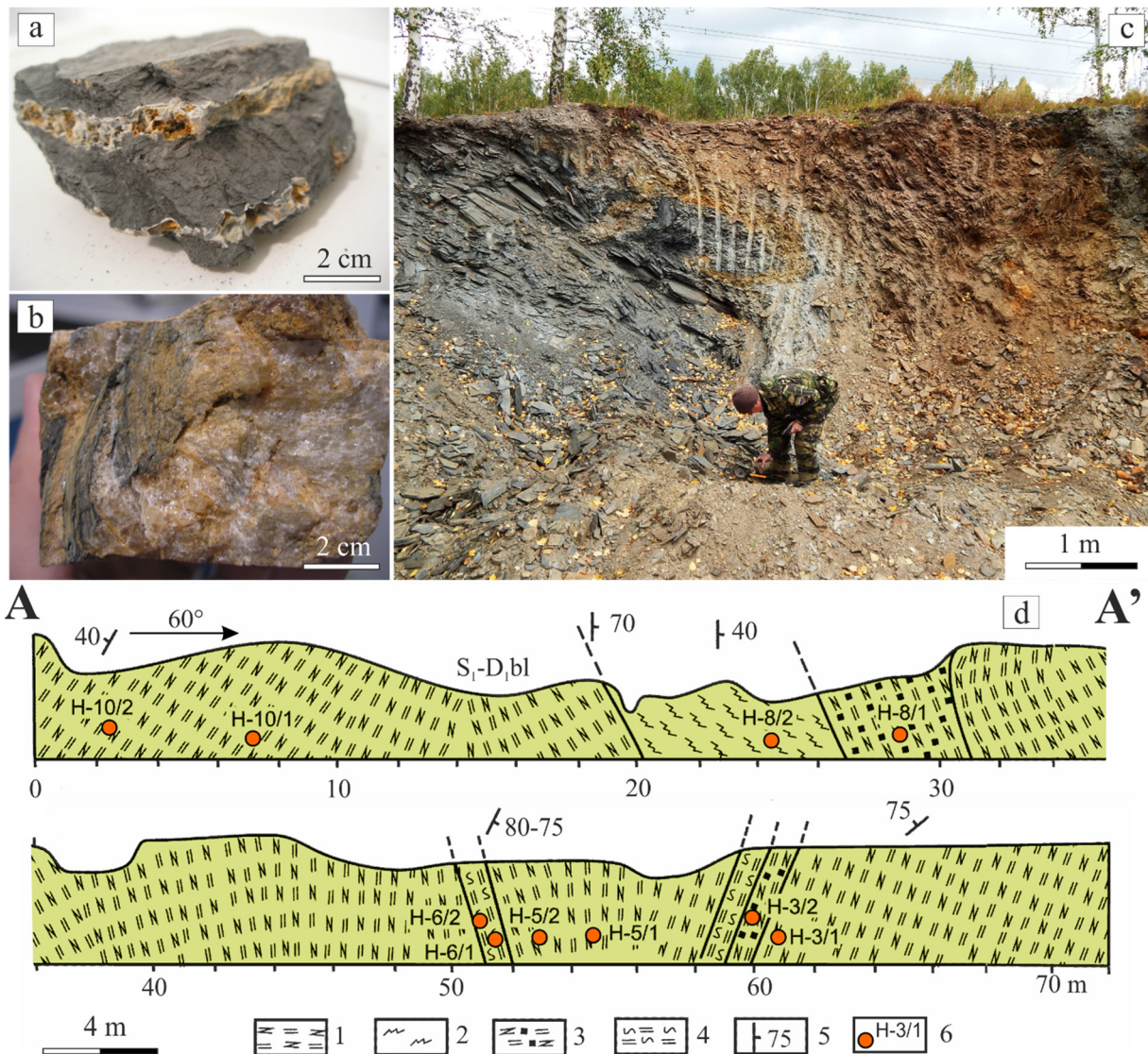


**Figure 13.** Typical sulfidized (a), silicified (b), and ferruginated (c) black shales and geological sections (d) [64] of the Bulatovo Formation along the bed of a stone quarry near the northern outskirts of the settlement of Nikolsky (see Figure 12a). Legend: 1—gray and dark gray carbonaceous–siliceous shales; 2—black flattened carbonaceous–clayey–siliceous shales, penetrated by a network of quartz veins; 3—brown ferruginated shales with limonitized pyrite; 4—light sericite–quartz shales; 5—elements of foliation and platy jointing; 6—samples with gold content (see Table 8).

**Table 8.** Gold contents in sulfidized and silicified carbonaceous sediments of the Larino dome framing (g/t) [59,64].

No.	Sample	Au	No.	Sample	Au	No.	Sample	Au
1	H-3/1	0.20	24	MC-1/2	0.54	47	9279-1	0.70
2	H-3/2	0.32	25	Lr-10	0.54	48	9279-5	0.27
3	H-5/1	0.19	26	Uv-1/2	0.30	49	9279-8	0.21
4	H-5/2	0.28	27	Uv-3/2	0.64	50	9279-10	0.30
5	H-6/1	1.93	28	Uv-3/3	0.59	51	9279-16	0.18
6	H-6/2	0.20	29	Uv-4/2	0.55	52	9280	3.60
7	H-8/1	1.66	30	Uv-5/2	0.53	53	9280-1	0.34
8	H-8/2	0.74	31	Nik-7/2	0.87	54	9280-2	0.20
9	H-10/1	0.17	32	Nik-7/3	0.55	55	9281	4.90
10	H-10/2	0.33	33	Nik-7/4	0.47	56	9281-1	0.21
11	H-24/1	1.12	34	Nik-9/2	0.47	57	9281-2	0.20
12	H-24/2	0.08	35	Nik-10/1	0.38	58	9285	0.10
13	H-25/1	0.15	36	Nik-10/2	0.51	59	9285-2	0.50
14	Pl-176/1	0.19	37	Nik-10/4	0.69	60	9285-3	0.10
15	Pl-5402-3	0.10	38	Nik-14/2	0.68	61	9285-4	0.40
16	Pl-5400-1	0.07	39	5524-2	0.43	62	9286	0.30
17	N-13/1	0.06	40	5529-2	0.42	63	9287	0.10
18	N-14/1	0.04	41	5529-18	0.71	64	294	0.24
19	N-14/2	0.11	42	5529-52	0.40	65	294-1	0.26
20	N-15/1	0.04	43	5530-180	0.49	66	294-2	0.05
21	N-16/1	0.12	44	Pl-11070	0.18	67	294-3	0.06
22	N-16/2	0.30	45	Pl-227	0.18	68	294-4	0.03
23	N-17/1	0.05	46	Pl-2715	0.34	69	5401-1	0.10

Notes: The analyses were performed using 1–43—VIMS (Moscow); 44–46—IGEM (Moscow); 47–69—fire assay procedure in the laboratory of JSC “Chelyabinskgeosyemka” (Chelyabinsk). The samples were taken from 1–16—a quarry near Nikolsky settlement; 17–23—former Proletarka village; 24–43—framing of the Larino dome; 44—a quarry near Novoustselimovo village.; 45—a section along the right bank of the Burlya river; 46—3 km north of Lesnoy settlement; 47–57—a quarry on the right bank of Mal. Uvelka river; 58–63—Suvatly town, north of Nikolsky settlement; 64–69—north of the Nikolsky settlement quarry.

Analysis of the obtained data revealed a distinct regularity of the location of elevated gold contents—all sites with industrial gold contents are located in the area of occurrence of the development of rocks of epidote–amphibolite and greenschale facies of metamorphism (Figure 12). The highest gold contents (Malouvelka, Nikolsky, and Pridannikovo occurrences) are confined to the epidote–amphibolite facies, the development of which is associated with the intrusion of granite massifs of the Varshava complex (Larino and Pridannikovo) and zones of intensive metasomatic transformation of rocks caused by the formation of subalkaline massifs of the Krasnokamensk complex near Nikolsky settlement.

It is noteworthy that within the amphibolite facies, there are no sites with gold contents higher than 0.1 g/t. The contents of this metal in these sites are either in the range of hundredths of grams per ton or within the sensitivity of the method (fire assay and X-ray spectral analysis with preliminary extraction). This indicates a significant removal of gold from the rocks of the immediate frame of the Larino granite–gneiss dome and confirms the correctness of the model of metamorphogenic–hydrothermal gold formation in the black shale strata of the Southern Urals that we are currently developing at [60]. It is worth noting that during the lithochemical survey of sheet N-41-XIII within the area under study, a complex geochemical anomaly (Ag, As, V, Mo, and W) was obtained [114]. This area is characterized by a wide development of brown iron ore formations associated with the rocks of the Bulatovo Formation, and numerous gold placers associated with them (the valleys of the Uzelganka and Kyshindyk rivers), which makes this node very promising for the discovery of rare metal mineralization and gold.

### 3.7. East Ural Megazone

The geological structure of the East Ural Megazone is complex and in places not quite unambiguously solved, which is due to the intense dislocation, uneven metamorphism of rocks and their poor exposure, and the presence of rare faunal remains. Carbonaceous shales within the Megazone are most widely developed in Carboniferous deposits.

The Tetechnaya Mountain occurrence combines several sites of gold mineralization discovered in a small tectonic block with a thickness of about 500–750 m (Figure 14). It is composed mainly of carbonaceous–siliceous shales with interlayers of polymictic sandstones and tuffaceous volcanogenic rocks. On the whole, the section is thin rhythmic with a flyschoidal-type appearance. Previously, the carbonaceous sediments were attributed to the black shale formation ( $C_1t_2-v_1$ ), but later, on the slope of Tetechnaya Mountain, graptolites, which are, in T.N. Koren's opinion, typical of the lower part of the Telychian substage of the Upper Llandovery *guerichi* zone (=linnaei or minor) [119], were collected in black siliceous–clay shales. When compiling the geological map of sheet N-40-XIII, these sediments were included in the Bulatovo Formation ( $S_1-D_1bl$ ) [114].

Quartz vein stockworks and zones of vein-disseminated sulfide mineralization, represented mainly by pyrite and chalcopyrite and less frequently by sphalerite, galena, and molybdenite, are widely developed there.

In the area under study, there are several points of gold mineralization belonging to the gold–sulfide–quartz ore formation type and located in the zones of tectonic disturbances and sulfidization among altered, stratified carbonaceous shales. Sampling of the latter of the contact of small bodies of porphyry diorites in the Birgilda–Tomino complex ( $\delta D_3-C_1bt$ ) showed up to 3.0 g/t Au (mineralization point Nos. 2 and 5, see Figure 14). In ferruginated shales and tuff sandstones with pyrite dissemination, Au contents reach up to 1.0 g/t (Figure 14, No. 1). In addition, studies of predecessors revealed an occurrence associated with the stockwork of quartz veins, with sulfide mineralization in berezitized and ferruginated tuff sandstones containing 1.8–9.6 g/t Au, 0.4–4.8 g/t Ag, and 0.4% Cu (Figure 14, No. 3).

The works of the Uvelka Geological Survey Team revealed gold mineralization in carbonaceous shales in the Tetechnaya Mountain area. A number of well cores were drilled there along three profiles and were up to 410 m deep (Figure 14b) [120]. Trench sampling of black shale and tuffogenic sedimentary rocks showed very encouraging results. According to 133 assay analyses, they contain gold in the range of 0.5–1.5 g/t (average 0.76 g/t) and silver up to 4.0 g/t (average 1.0 g/t) (Table 9). Geochemical anomalies of antimony (3–5 g/t) and silver (0.4–1.0 g/t) are also located in the area of development of carbonaceous sediments.

A 1:50,000 scale geological survey carried out on black shale rocks identified a gold-bearing weathering crust (No. 4, Figure 14) [114]. As a result of trench sampling of core holes by the fire assay procedure, elevated gold contents were revealed in volcanogenic–sedimentary rocks. The gold content in them (mainly native—sulfides are completely oxidized) ranges from 0.3 to 3.0 g/t. The increased gold concentrations occur in the lower and middle parts of the clay–rubble horizon of the weathering crust, from which we washed and studied several 0.05–0.2 mm gold particles. The particles have low fineness (664–754) and contain silver in the amount of 15.38–33.58 wt.%. The gold particles were found to contain an insignificant admixture of bismuth (up to 0.29%), osmium, and iridium (up to 0.25%).

The studied prospect, the industrial analogs of which are well known in many folded areas, is not of industrial interest yet because of its poor exploration. However, according to a number of features, it may turn out to be quite profitable for development in the near future.

The Kamenka area is part of the Alapaev–Chelyabinsk deep fault zone and represents a key-shaped structure of alternating grabens and horsts composed of volcanogenic–sedimentary rocks of the Devonian and Carboniferous ages (Figure 15). Carbonaceous sediments are widely represented in the Birgilda Formation penetrated by the intrusive bodies of the Birgilda–Tomino complex [121].

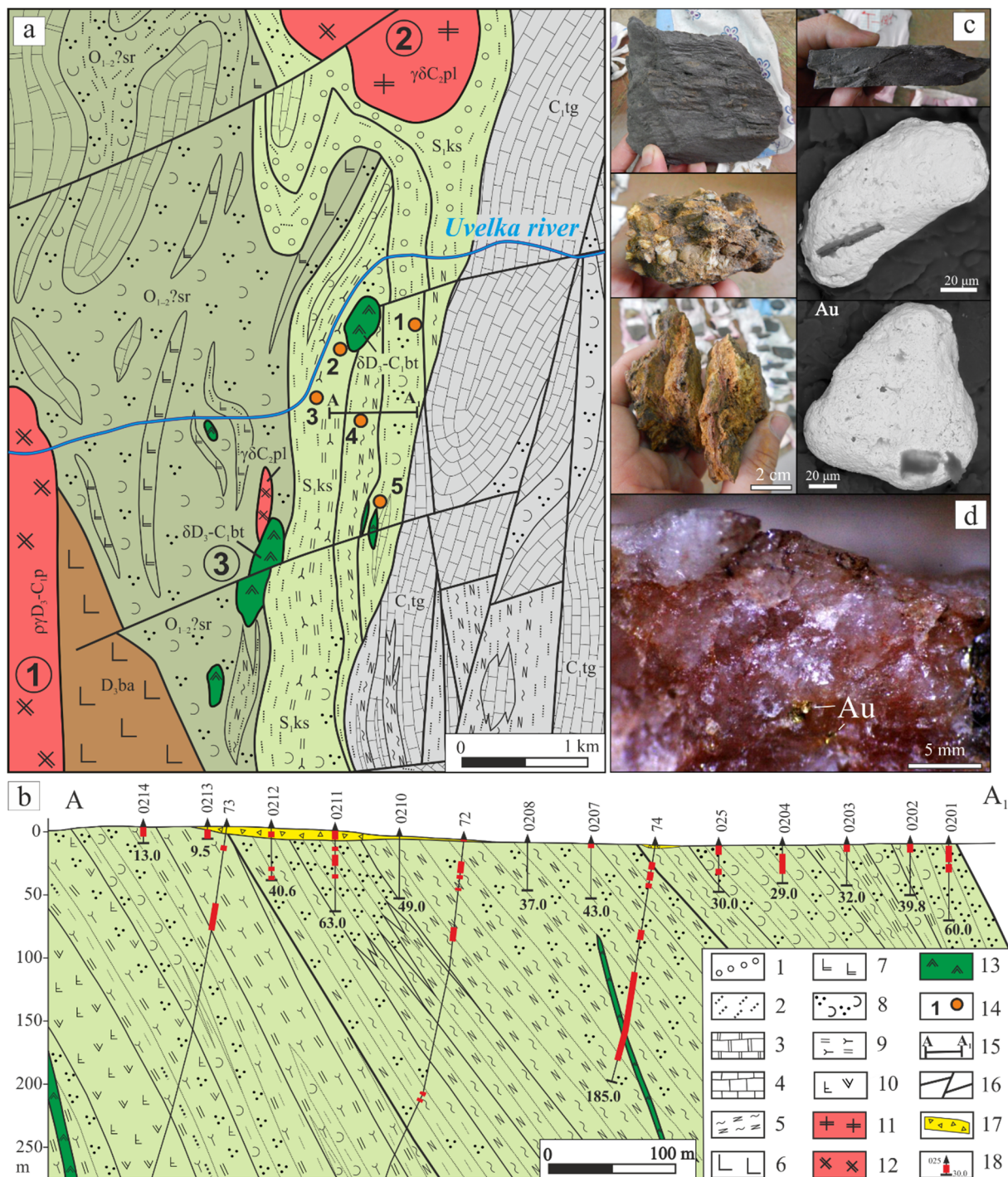


**Figure 14.** Geological map (a), cross-section (b), typical carbonaceous shales (c), and native gold (d) of the Tetechnaya Mountain occurrence ( materials from E.P. Shchulkin and [120] with the authors’ modifications). Legend: 1—polymictic conglomerates, 2—sandstones, 3—marbleized limestones, 4—limestones, 5—carbonaceous clay shales, 6—andesibasalts and their tuffs, 7—microporphyrites of basalt composition, 8—interlayering of siltstones and tuffs of andesite composition, 9—siliceous tuffs, 10—plagioclase porphyrites of andesite–basalt composition, 11—biotite granites, 12—biotite diorites, hornblende, 13—quartz–plagioclase dacites, 14—Au mineralization points and their numbers, 15—line of the cross-section A-A1 on wells, 16—faults; 17—weathering crusts, 18—wells, their numbers, depth, and sampling interval. Figures in circles are numbers of intrusive massifs: 1—Koelga, 2—Uvelka, 3—Zelenodol.

**Table 9.** Results of trench sampling for Au and Ag in black shale and tuffogenous–sedimentary rocks of the Kosobrodka Formation (g/t) [120].

No.	Well No.	Depth (m)	Au	Ag	No.	Well No.	Depth (m)	Au	Ag
1	U-0207	0.0–3.0	0.3	0.3	33	U-72	71.0–72.0	0.7	1.0
2	U-0212	31.0–32.0	0.6		34	U-72	73.0–74.6	1.5	1.0
3	U-0212	40.0–40.5	0.5		35	U-72	74.6–76.0	0.3	1.2
4	U-0212	3.0–5.0	0.7	0.7	36	U-72	77.5–79.0	0.3	0.8
5	U-0212	5.0–7.0	0.8		37	U-72	91.0–92.5	0.3	1.0
6	U-0211	0.3–5.5	0.6		38	U-72	198.6–200.1	0.3	1.1
7	U-0211	7.5–9.0	0.6		39	U-72	204.9–206.4	0.4	1.4
8	U-0211	13.0–15.0	0.3		40	U-72	210.5–211.9	0.3	0.9
9	U-0211	19.0–27.0	0.5		41	U-72	278.2–281.1	0.6	1.3
10	U-0211	35.0–37.0	0.3		42	U-74	15.0–17.3	0.5	
11	U-0201	1.5–14.7	0.4	0.3	43	U-74	18.5–20.0	1.2	
12	U-0201	18.0–23.0	0.3		44	U-74	22.2–23.2	0.4	0.9
13	U-0202	0.0–3.7	0.7	0.3	45	U-74	23.2–24.2	0.4	1.6
14	U-0203	0.0–5.0	0.5	1.0	46	U-74	24.2–25.4	0.3	1.3
15	U-0205	0.05–3.0	0.8	4.0	47	U-74	27.4–28.4	0.4	0.4
16	U-0204	7.0–19.0	0.5		48	U-74	28.4–29.5	0.6	1.0
17	U-0213	2.0–9.5	1.0		49	U-74	32.0–33.5	0.7	0.8
18	U-0214	0.1–7.0	0.4		50	U-74	66.6–68.0	0.5	1.0
19	U-73	16.0–18.8	0.4	0.6	51	U-74	73.5–74.9	0.5	1.0
20	U-73	60.5–62.3	0.6	0.4	52	U-74	105.5–107.0	0.3	1.6
21	U-73	79.4–80.7	1.4	0.8	53	U-74	111.5–112.8	0.3	1.2
22	U-72	5.8–7.8	0.4	0.6	54	U-74	122.5–124.0	0.5	1.2
23	U-72	16.8–20.8	0.5	0.7	55	U-74	125.5–127.0	0.6	1.6
24	U-72	20.8–21.8	0.5	0.8	56	U-74	127.0–128.5	0.3	1.2
25	U-72	21.8–22.8	0.4	0.6	57	U-74	128.5–130.0	0.3	0.8
26	U-72	22.8–23.8	0.3	0.8	58	U-74	131.5–132.5	0.6	1.5
27	U-72	23.8–24.8	0.4	0.8	59	U-74	135.0–136.8	0.4	1.0
28	U-72	24.8–25.8	0.3	0.6	60	U-74	137.8–139.3	0.4	0.8
29	U-72	27.8–28.8	0.3	0.8	61	U-74	144.7–146.0	0.8	1.0
30	U-72	28.8–30.0	0.5	0.6	62	U-74	146.0–147.0	1.0	1.2
31	U-72	39.5–41.0	0.3	1.0	63	U-74	156.6–158.1	0.6	1.0
32	U-72	69.5–71.0	0.4	1.0	64	U-74	159.6–161.6	0.3	1.0

Note: 1–5—clayey–carbonaceous sandstone, 6—fine-grained sandstone, 7–15—siltstone, 16—tuff siltstone, 17–18—sericite–siliceous, phyllitized tuffite, 19–21—siliceous tuffite of dacite composition, 22–23—clayey siltstone, 24–31—clayey–carbonaceous sandstone, 32–36—clayey–carbonaceous sandstone, sulfidized, 37–41—clayey siltstone, 42—fine-grained sandstone, 43–46—siltstone, 47–48—clayey–carbonaceous sandstone, 49–52—siliceous carbonate–sericite–feldspar metasomatite, 53–64—carbonaceous sericite–carbonate siltstone. The analyses were obtained using an assay method by the Uvelka Geological Survey Team (Chelyabinsk).

The Birgilda Formation (C<sub>1</sub>bg) is composed of white and gray organogenic limestones (frequently marbled near the contacts with intrusive massifs) with interlayers of carbonaceous–clayey, calcareous–clayey shales, and siltstones forming independent beds and horizons (Figure 15). The thickness of the strata is about 700 m. The alternation of coarse-, medium-, and fine-clastic rocks throughout the section shows a transgressive character, and the presence of carbonates in the section indicates their formation in the shallow and coastal shallow water area of the sedimentary basin. The Visian–Serpukhovian age of the formation is accepted on the basis of the foraminifer and conodont fauna found in it. The absolute age of diorites of the Birgilda–Tomino complex corresponds to the Late Devonian–Early Carboniferous, but recently, data on their Silurian age have been obtained [122].

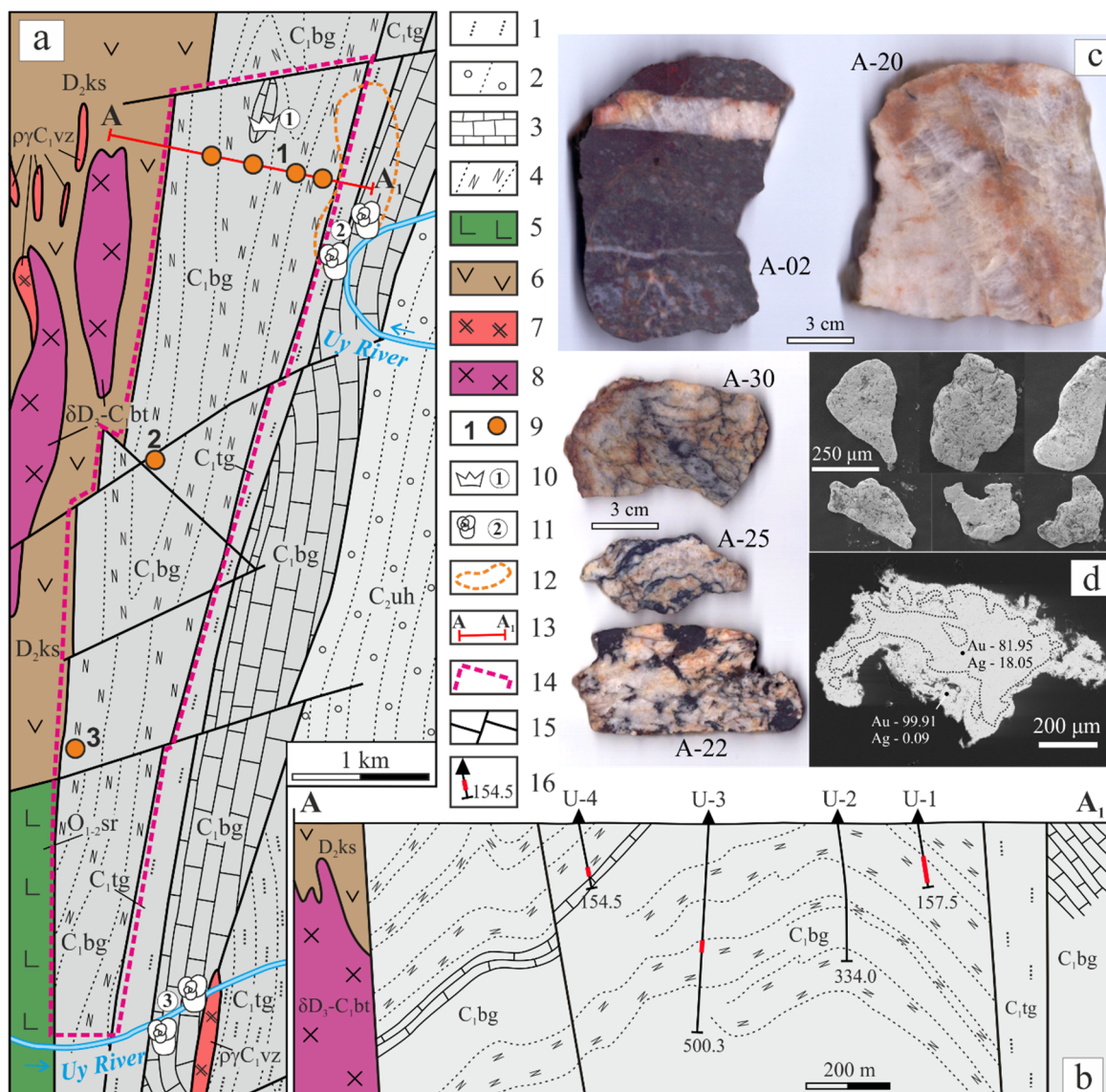


**Figure 15.** Geological map (a), cross-section (b), typical carbonaceous shales of the Birginda Formation (c), and native gold of the Kamenka area (d) (based on the materials of E.P Shchulkin [121]). Legend: 1—sandstones; 2—conglomerates; 3—limestones; 4—carbonaceous shales; 5—basalts; 6—andesites and their tuffs; 7—plagiogranites; 8—diorites, quartz diorites; 9—significant gold contents; 10—sites of finding conodonts; 11—sites of finding foraminifera; 12—area favorable for the identification of placer gold; 13—line of the cross-section A-A<sub>1</sub>; 14—outline of the Kamenka area prospective for gold; 15—faults; 16—wells, their numbers, depth, and sampling interval (see Table 10). The dashed line on the gold particle shows the boundary of the high fineness hypergene rim.

Carbonaceous sediments of the Birgilda Formation are a favorable environment for the localization of noble metal mineralization. Metamorphogenic gold ore occurrences are found in a 5 × 2 km tectonic block, which is a narrow anticlinal fold composed predominantly of carbonaceous carbonate–terrigenous sediments. A large number of deep cores were drilled by the Chelyabinsk geological prospecting expedition of Uralgeologiya, which allowed clarification of the geological structure of the area and identification of a number of promising prospects [114].

**Table 10.** Results of trench sampling for Au and Ag in the black shale from the Birgilda Formation (g/t) [121].

No.	Well No./Depth (m)	Au	Ag
1	U-3/280.0–295.6	0.4	6.2
2	U-1/56.0–57.0	1.6	-
3	U-1/84.4–93.2	0.7	-
4	U-1/101.0–118.0	0.5	11.0
5	U-1/130.6–135.8	1.3	-
6	U-3/275.9–278.0	3.0	-
7	U-4/99.6–103.1	2.0	1.7

Note: The dash is the content below the detection limit. The analyses were obtained using the assay method by the Uvelka Geological Survey Team (Chelyabinsk).

Occurrence No. 1 was in the trench samples, and the analysis indicated high gold contents of up to 3.0 g/t and silver contents of up to 11.0 g/t (fire assay method) (Figure 15, No. 1). The maximum content of noble metals occurs in the interlayers of gray and dark gray carbonaceous shales with a thickness from 60 to 150 m (Figure 15, Table 10). They contain rare low thin (0.5–6.0 cm) quartz–carbonate veins, cutting the schistosity and carrying thin phenocrysts of pyrite and chalcopyrite up to 4%.

Occurrence No. 2 was in the contact zone of the porphyry diorites of the Birgilda–Tomino complex, and the contents of noble metals are even higher (Figure 15, No. 2). Sampling of intensely silicified and sulfidized carbonaceous sediments showed Au contents up to 4.6 g/t. An area-wide geochemical anomaly of arsenic up to 0.02% is noted throughout the carbonaceous shale development area; spectral analysis revealed elevated contents of copper—0.1%, zinc—0.01%, and barium—0.07%.

Occurrence No. 3 was as follows. Mineralization similar to the first occurrence was noted in the southern part of the area. A one-meter zone with poor sulfidization (up to 1%) and up to 0.3 m thick quartz veins was identified in weakly carbonaceous gray quartz–chlorite–sericite schists. The fire assay analysis showed that gold contents are 1.6 g/t and silver contents are 5.0 g/t.

During the latest geological survey work, carbonaceous shales of the Birgilda Formation, as well as their silicified and ferruginated varieties, were tested for gold and silver (Table 11). The analysis showed stable above-background contents of precious metals, reaching industrial contents in some of the samples.

**Table 11.** Results of pit sampling for Au and Ag in the black shale from the Birgilda Formation (g/t) [121].

No.	Sample	Au	Ag	No.	Sample	Au	Ag
1	A03	0.03	0.17	15	A02	0.09	0.09
2	A05	0.16	0.21	16	A08	0.39	0.59
3	A06	0.13	0.46	17	A09	0.66	0.48
4	A07	0.14	5.10	18	A12	-	0.16
5	A10	-	0.21	19	A13	0.13	0.22
6	A11	-	0.19	20	A14	0.06	0.34
7	A15	0.19	0.18	21	A16	0.03	0.16
8	A17	0.14	1.02	22	A18	0.19	0.15
9	A19	0.09	0.11	23	A20	0.21	0.09
10	A23	0.06	0.15	24	A21	0.12	0.53
11	A24	0.18	0.15	25	A22	0.17	0.11
12	A26	0.08	0.17	26	A25	0.10	0.82
13	A27	0.19	0.19	27	A28	0.23	0.18
14	A29	0.14	0.14	28	A30	0.12	0.42

Note: 1–15—carbonaceous shales, 16–28—silicified and ferruginated rocks on shales. Dash—the content of the element is below the sensitivity threshold of the analysis. The analyses were carried out at the Institute of Geology UFRS RAS (Ufa) using the atomic absorption method.

During the geological and survey work, we sampled the Neopleistocene weathering crusts consisting predominantly of yellowish-brown loams and clays with fragments of veined quartz and carbonaceous shale. In the process of washing the samples in a wash pan, we obtained several small gold particles in the form of thin flakes of  $0.2 \times 0.4 \times 0.4 \times 0.01$  mm in size and isometric medium-sized particles with sizes of  $1 \times 1.5$  mm and  $0.5 \times 1$  mm (weighing 10 and 2 mg, respectively) (Figure 15). Judging by the shape of the gold particles, the metal was transferred to a short distance from the primary source, which could be zones of quartz–sulfide mineralization, as well as carbonaceous–clay shales of the Birgilda Formation.

Microprobe analysis showed a heterogeneous composition of gold (part of it is high fineness gold), which indicates its relationship with quartz veins (gold–quartz type) [121]. Some gold particles contain significant amounts of silver (up to electrum) and copper (copper and high-fineness copper gold [123]), which suggests that they can be attributed to the gold–sulfide type and are most likely related to the carbonaceous–clay shales of the Birgilda Formation.

Coarse gold is heterogeneous and has hypergenic neomineralization represented by high fineness rims, while the difference in silver content between the central and marginal parts can be 26 wt.%. The development of such rims was numerously reported for gold particles from a number of deposits of the Southern Urals [95,124,125] and is associated with both chemical refining of gold particles from impurity elements in the hypogene zone [126] and recrystallization of deformed sections of grains [127]. The depth of development of the high fineness rim is rather large and is about 100–150 microns, which indicates an extended time of residence of gold particles in the zone of hypergenesis [128].

Carbonaceous shales of the Birgilda Formation have noble metal speciation. In sulphidized and tectonically altered rocks, gold and silver contents reach commercial concentrations, which raises hopes of discovering a new gold object within the Kamenka area.

The Kumak ore field is confined to the Early Carboniferous Anikhov graben of the East Ural uplift, which is composed of carbonaceous–carbonate–terrigenous sediments. In the central part of the graben, a chain of gold deposits and occurrences confined to the Bredy Formation (C<sub>1</sub>bd) stretches for tens of kilometers along the strike (Figure 16). Numerous prospecting–exploration and thematic works carried out here for almost a century allowed for the clarification of the geology of the ore field and conducting metallogenic constructions and reconstructions of the conditions for sediment accumulation [4,129–136].

The Bredy Formation within the area under study is represented by sericite–quartz–carbonaceous and quartz–carbonaceous–tourmaline fine-grained shales with weakly pronounced schistosity and easily cleavable on planes with angular fractures. Sandstones, conglomerates, siltstones, limestones in subordinate quantities, and horizons of basic volcanics are also observed. The age of its sediments is determined from the finding of foraminifera in limestone interbeds, and the thickness of the formation is 350–700 m. At depth, carbonaceous shales are penetrated by an intrusion of quartz diorites of the Kumak complex ( $\delta C_1 k$ ), extending along the entire ore zone. The diorites are broken down schistose and frequently have no clear boundaries with the host rocks [137].

The Kumak ore field is characterized by a wide variety of gold mineralization and a complex polygenetic type of mineralization [138]. The mineralization occurs in the beds of metamorphosed primary terrigenous and clayey rocks transformed into carbonaceous micaceous–quartz and quartz–carbonate–mica chloritized shales. Four mineral associations are gold bearing in the Kumak ore field [139]. The first of them, developed only in the south of the ore field, is represented by tetradymite and native gold. The second, fine-grained native gold, is developed in the fractures filled with flake chlorite and sericite and, less often, with scheelite. The third association, poorly manifested within the area, is polymetallic mineralization, with a low content of noble metals. The fourth one occurs in the main zone of the crush in the northern section and is predominant. Gold here is finely dispersed, associated with small crystals of pyrite and arsenopyrite, and occurs in the areas of abundant tourmalinization (Figure 17).

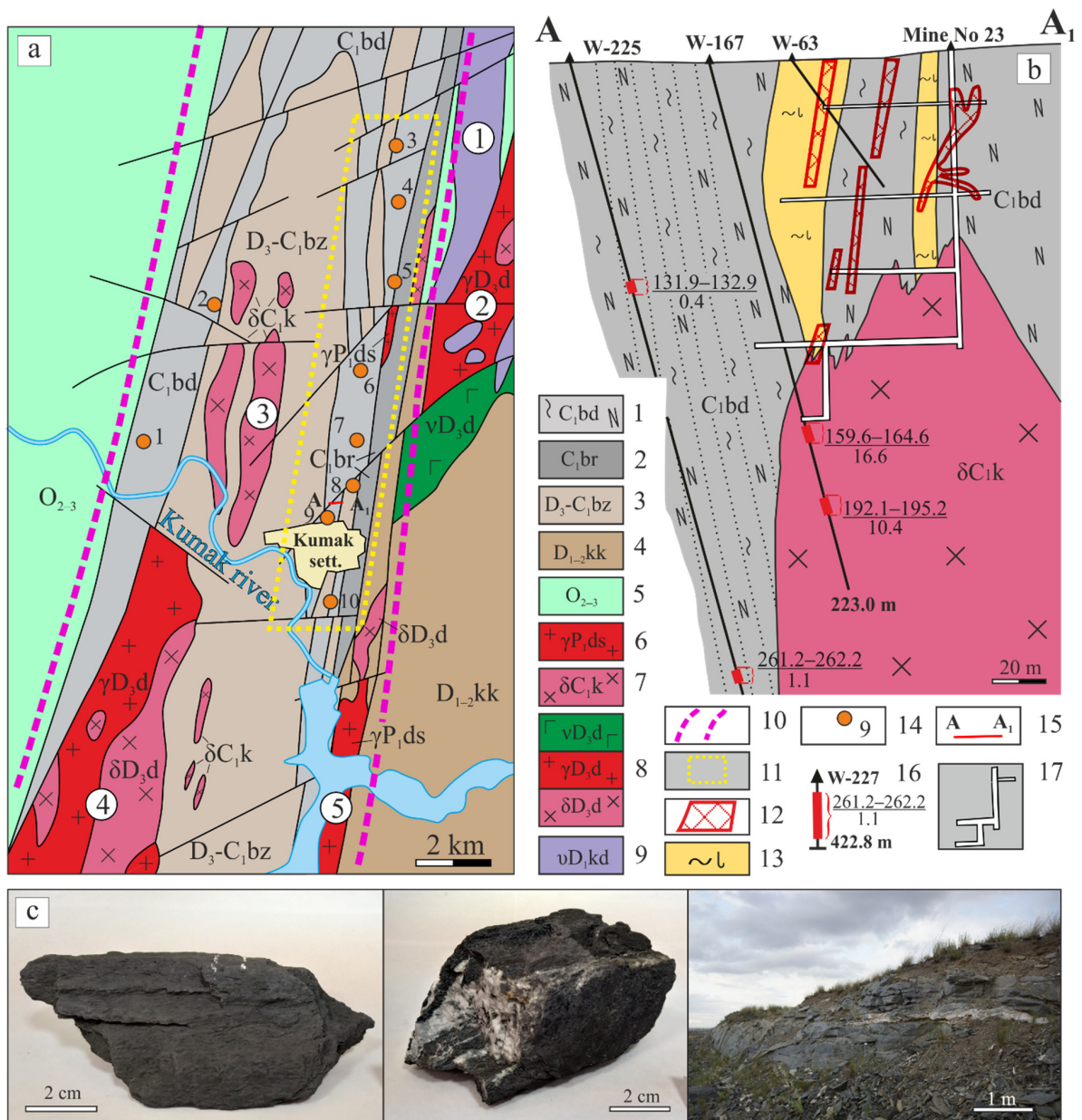


**Figure 16.** Geological map (a), cross-section (b) of the Kumak ore field and carbonaceous shales and quartz veins (c) of the Kumak deposit ([137] with authors’ simplifications). Legend: 1—Bredy Formation (carbonaceous shales, sandstones, siltstones); 2—Birgilda Formation (conglomerates, sandstones, limestones); 3—Bereznik Formation (tuffs of basic and acidic composition, interlayers of siltstones); 4—Kokpektin Formation (lavas and tuffs of basalts); 5—Enbekshinsk Formation (basalts, shales); 6—Dzhabyk–Sanar granite–leucogranite complex; 7—Kumak diorite–plagiogranite complex; 8—Dzhabygasai diorite–plagiogranite–gabbro complex; 9—Kamenodolsk ultramafic complex; 10—boundaries of the Anikhov graben; 11—boundaries of the Kumak ore field; 12—contours of ore bodies; 13—ore-bearing quartz–mica–tourmaline metasomatites by carbonaceous shales; 14—gold occurrences and deposits: 1—Khishchnik, 2—Tamara, 3—Ermak, 4—Vostochno-Tykashinskoye, 5—Kommercheskoye, 6—Zabaikalskoe, 7—Baikal, 8—Tsentralnoye, 9—Kumak, 10—Kumak–Yuzhny; 15—line of the cross-section A–A<sub>1</sub>; 16—wells, their depth, sampling interval, and gold content (g/t); 17—mines and adits. Intrusive massifs (numbers in circles): 1—Kayraktinsky, 2—Dzhabygasai, 3—Tykashinsky, 4—Akzharsky, 5—Kumak dike.

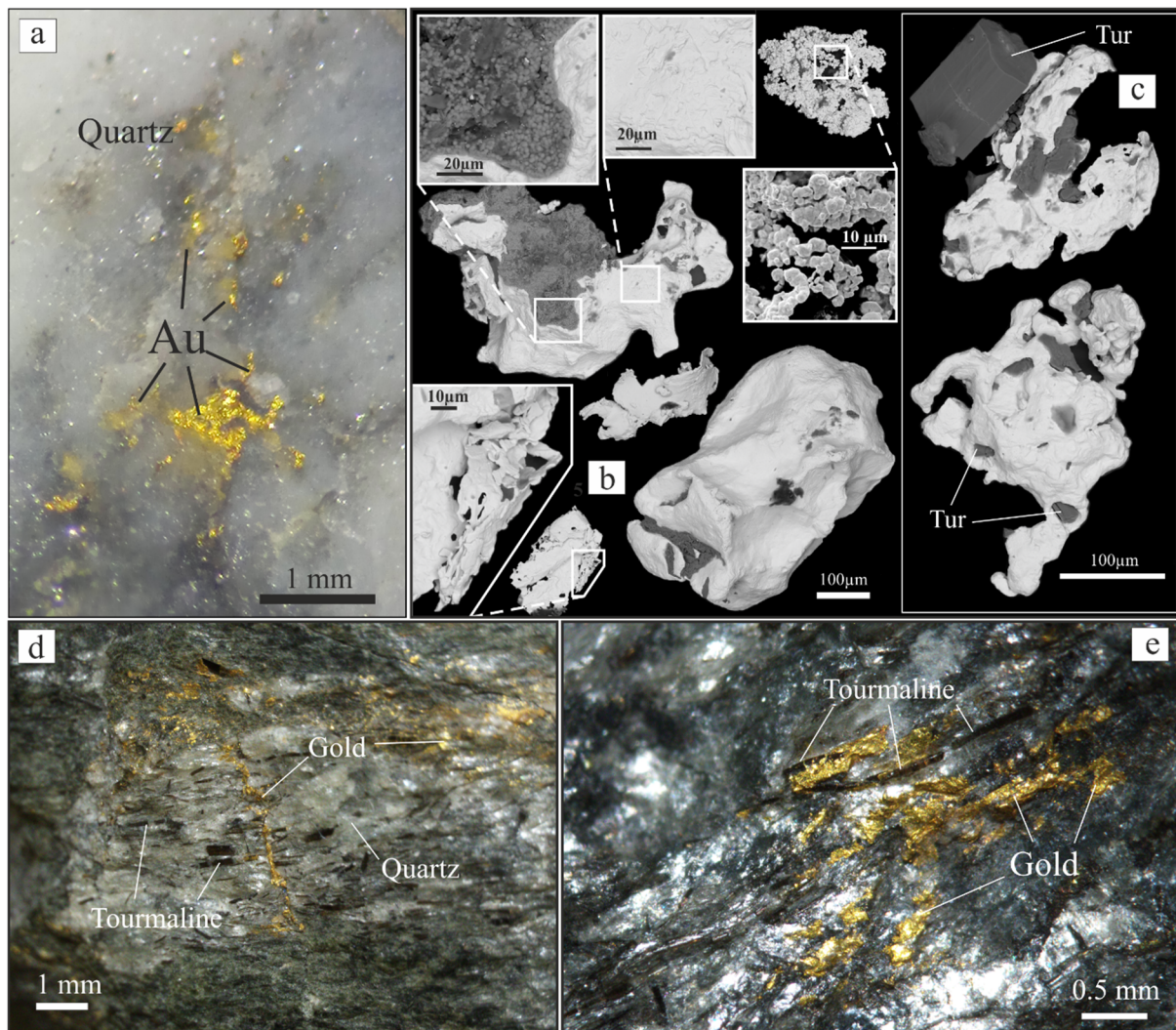


**Figure 17.** Photo and electron microscope images of gold from the Kumak and Baikal deposits. Visible gold in quartz veins (a); gold flakes from silicified carbonaceous shales and weathering crusts (b); close intergrowth of tourmaline and gold in carbonaceous shales (c–e). Samples (d,e) are stored in the Museum of Geology and Mineral Resources of the Republic of Bashkortostan (Ufa city).

Tourmaline is separated in the form of idiomorphic crystals of a short-columnar and prismatic shape, 0.1 to 0.3 mm in size. It is distinctly pleochroic from dark green to light green and often exhibits a zonal structure highlighted by coloration. According to chemical composition, tourmalines belong to dravite, foitite, and schorl [133]. They are high magnesian, do not contain impurities of Mn, F, and As, metals typical of tourmalines from porphyry deposits and granites [140–142], and are similar to the metamorphogenic dravite of orogenic gold and gold–sulfide deposits, as well as the tourmaline of gold–porphyry prospects [143–145]. This indicates the synchrony of their deposition and allows distinguishing a quartz–tourmaline gold-bearing formation within the Kumak ore field, which is comparable to some prospects in Eastern Transbaikalia and Tuva [130,146,147]. The most probable source of tourmaline mineralization in sericite–quartz–carbonaceous shales is boron-bearing marine sediments saturated with clay particles that underwent metamorphic transformation [145,148,149].

During fieldwork at the Kumak deposit, slightly altered and altered carbonaceous shales of the Bredy Formation were tested for gold and silver (Table 12). In the former, the Au content reaches 0.6 g/t and that of Ag 3–4 g/t. In the altered shales, the distribution of Au is extremely uneven—from 0.1 to 17.7 g/t. In general, the analysis showed stable

above-background contents of noble metals in black shales, reaching industrial contents in a number of samples.

**Table 12.** Results of Au and Ag pit sampling of quartz veins and quartz–mica–tourmaline carbonaceous sediments from the Kumak deposit (g/t) [132,136].

No.	Sample	Au	Ag	No.	Sample	Au	Ag	No.	Sample	Au
1	KM008s	0.15	-	18	KM028g	0.12	-	35	KM01s	0.28
2	KM010s	-	-	19	KM038s	-	-	36	KM02s	0.10
3	KM011g	3.50	-	20	KM005s	-	3.9	37	KM03s	0.34
4	KM012s	-	-	21	KM014s	0.15	-	38	KM04s	0.15
5	KM001g	6.50	-	22	KM019s	-	2.9	39	KM05s	0.12
6	KM004s	-	-	23	KM023g	-	3.2	40	KM06s	>20.00
7	KM004g	0.64	-	24	KM032s	-	3.3	41	KM07s	0.14
8	KM005s	-	-	25	KM009s	0.55	-	42	KM08s	0.16
9	KM006s	-	-	26	KM015g	0.15	4.1	43	KM09s	0.20
10	KM020s	-	-	27	KM024g	-	3.2	44	KM10s	0.12
11	KM046s	0.15	-	28	KM025s	-	-	45	KM11s	0.11
12	KM006g	0.25	-	29	KM026s	-	-	46	KM12s	0.17
13	KM010g	0.79	-	30	KM031s	-	3.0	47	KM13s	0.13
14	KM012g	0.32	-	31	KM037s	0.20	2.5	48	KM14s	0.16
15	KM013g	0.57	-	32	KM044s	-	4.0	49	KM15s	0.14
16	KM021g	-	-	33	KM048s	0.28	2.5	50	KM16s	0.16
17	KM022g	17.70	-	34	KM049s	0.19	3.0	51	KM17s	-

Note. 1–4—quartz veins; 5–51—black shales: 5–19—silicified ferruginated, 20–51—weakly altered carbonaceous shales. Silver was not determined for Nos. 35–51; dash—the element content is below the sensitivity of the method. Determinations of noble metals were carried out in the laboratory of LLC “Orenburg Multiprofile Company” using the extraction–atomic absorption method with organic sulfides (Orenburg, analyst A.I. Korchagina) (Tables 12 and 13).

In the central part of the Baikal deposits, we have described and sampled a section that fully exposes the ore-bearing black shale band. Pit sampling of all varieties of rocks in the section and the area of the occurrence showed commercial contents of gold (up to 6.5 g/t) and consistently high concentrations of silver (up to 7.6 g/t) (Table 13).

**Table 13.** Results of analysis for Au and Ag silicified and ferruginated black shales of the Baikal deposit (g/t) [134].

No.	Sample	Au	Ag	No.	Sample	Au	Ag	No.	Sample	Au	Ag
1	km85g-1.0	0.09	3.4	10	km85s-80.4	0.18	2.0	19	km85s-29.0	0.08	1.4
2	km85g-4.0	-	3.2	11	km85s-100.0	-	1.8	20	km85s-30.0	-	1.4
3	km85g-11.4	0.15	3.4	12	km85s-105.0	0.09	2.2	21	km85s-40.0	0.09	1.0
4	km85g-35.6	0.15	7.2	13	km85s-21.1	0.44	1.8	22	km85s-66.0	0.10	2.0
5	km85g-42.8	0.06	3.4	14	km85g-29.2	0.12	3.0	23	km85s-75.0	0.16	1.4
6	km85g-48.3	0.06	2.6	15	km85s-55.0	0.09	2.6	24	km85s-90.0	0.09	0.8
7	km85g-60.3	0.08	4.2	16	km85g-96.3	0.09	1.8	25	km85s-70.0	0.35	2.4
8	km85s-67.7	0.15	1.6	17	km85g-102.8	0.08	2.6	26	km85g-86.5	0.08	3.4
9	km85g-72.0	0.07	7.6	18	km85s-25.0	0.06	2.2				

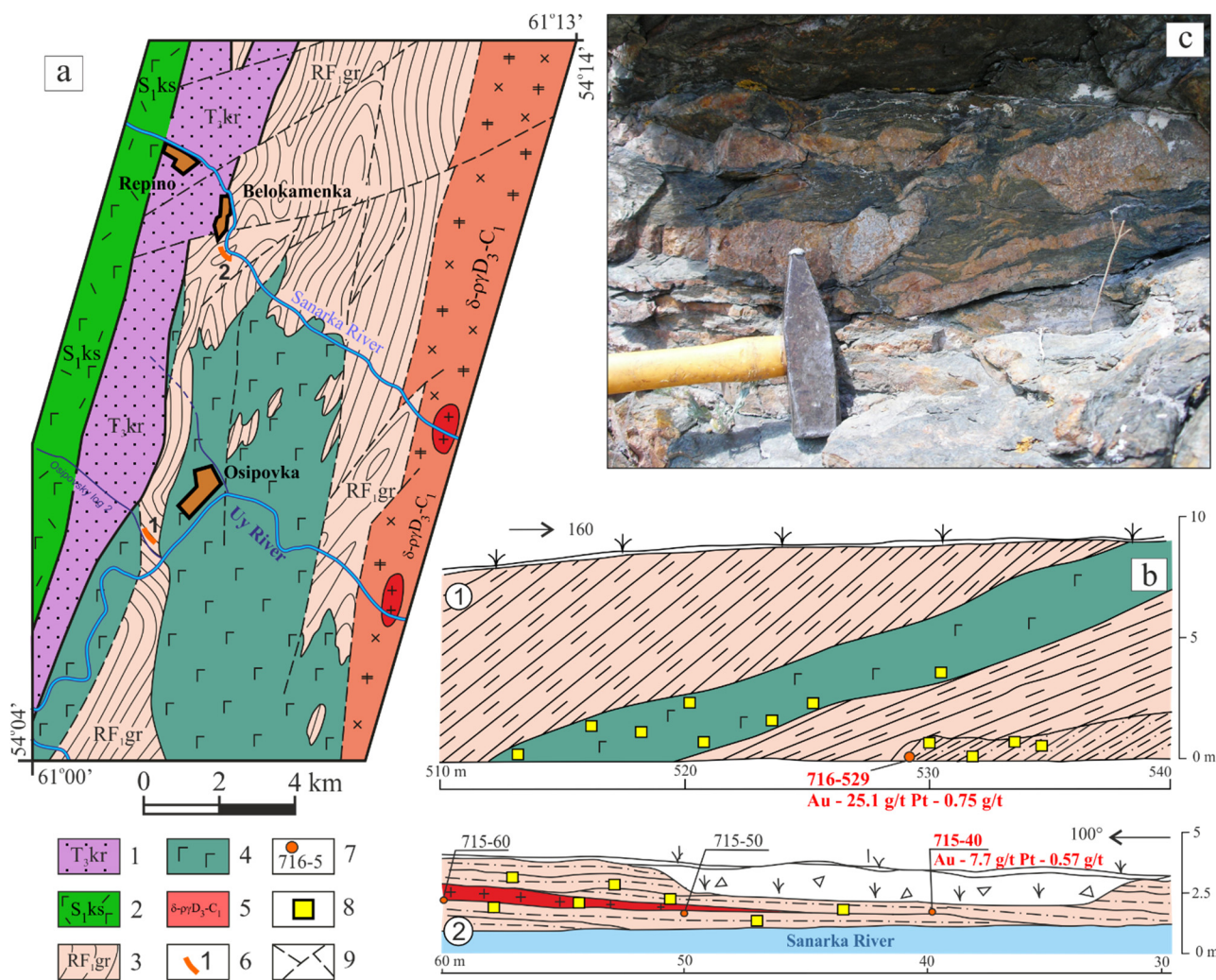
Note: 1–12—gray sericite shale; 13–17—black carbonaceous shale; 18–24—vein quartz; 25—vein quartz, porous, ferruginated; 26—light, ferruginated gray carbonaceous shale; dash—element content below the sensitivity of the method.

Taking into account the extremely irregular gold content in the ore bodies, we additionally washed samples from carbonaceous shales and weathering crusts, consisting mainly of weathered rock and fragments of vein quartz and carbonaceous shales, and also analyzed the crushed samples (Figure 17). In total, about 40 small gold particles ranging in size from  $0.05 \times 0.1$  to  $0.3 \times 0.1$  mm were obtained. A visible cluster of gold, penetrating the sample deep into a depth of 1.5 cm, was also found in a quartz veinlet. The forms of native gold occurrence are diverse and include lamellar and isometric in the form of intergrowths and leaflets (Figure 17).

Collomorphic kidney-shaped crusts of limonite and aggregates with muscovite and tourmaline are often observed on the surface of the gold particles. Microprobe analysis showed their fairly homogeneous elemental composition. Gold belongs to the high fineness type (Au—90–96 wt.%), and silver content is 4–9 wt.%. It is noteworthy that on some of them, a secondary redeposition of gold takes place in the form of small spongy high-fineness outgrowths, which is characteristic of the supergene or hypogene zone.

### 3.8. Trans-Ural Uplift

The Osipovka gold deposit is located within the Trans-Ural Uplift in the western frame of the large Nizhnesanar granite massif and is bounded by carbonaceous sediments of the Lower Riphean Gorodishche Formation (RF<sub>1</sub>gr) (Figure 18).



The formation is developed in the form of isometric belts stretching from south to north, and it is in the form of large tectonic blocks in the central part of the territory. Thick interbeds of graphitic quartzites occur among green feldspar–amphibole, epidote–chlorite–amphibole schists, amphibolites, and metabasalts. The sediments of the Gorodishche Formation are intensely metamorphosed and fragmented, silicified and sulfidized, and penetrated by numerous dikes of different compositions (from gabbro–diabases to plagiogranites). The lower contact of the formation is unknown. According to the data of the geologists of JSC “Chelyabinskgeosmoteka”, the sediments of the formation with stratigraphic disconformity are overlapped by the deposits of the Alekseevka Formation. The age of the Gorodishche Formation is assumed to be Early Riphean on the basis of findings of microphytoliths and nelkanellae *Osagia tenuilamellata* Keitl. and its comparability with similar strata, whose ages were determined by radiological methods. The thickness of the formation is 1000–2400 m.

They are well exposed for 800 m in the valley of the Osipovska Log creek (Figure 18a), which flows into the Ui river. Analysis of the pit and trench samples from black shale deposits showed industrial gold contents in them (average for 12 samples is 2.75 g/t, maximum is 25.1 g/t) and 0.750 g/t platinum (Figure 18, Table 14) [150]. One of the samples, 716/529, contains a gold particle that is 1.5 × 1.0 mm in size.

**Table 14.** Contents of noble elements in pit and trench samples of rocks from the Gorodishche Formation (g/t) [150].

No.	Sample	Au	Ag	Pt	Pd
1	5012	0.05	0.23	0.22	0.04
2	5013	0.06	0.39	0.27	0.04
3	5013/1	0.02	3.82	0.19	0.03
4	5001/78	<0.004	8.70	0.16	0.04
5	715-40	7.70	0.46	0.57	0.05
6	716-529	25.1	0.69	0.75	0.11
7	5002-107	0.11	0.67	0.35	<0.01
8	5002-362	0.01	0.25	0.53	0.04
9	5050-27	0.01	0.42	0.05	<0.01
10	5050-39	0.0039	0.34	0.03	<0.01
No.	Sample	Au	No.	Sample	Au
11	bk-01	0.08	20	os-01	0.05
12	bk-02/1	0.08	21	os-02	0.08
13	bk-02/2	0.08	22	os-03	0.06
14	bk-03/1	0.10	23	os-04	0.01
15	bk-03/2	0.13	24	os-05	0.03
16	bk-04/1	0.04	25	os-06	0.03
17	bk-04/2	0.03	26	os-07	0.05
18	bk-04/3	0.02	27	os-08/1	0.07
19	bk-05	0.21	28	os-08/3	0.02

Note: The samples were analyzed using atomic absorption analysis with preliminary extraction at the Analytical Certification Testing Center of the Russian Research Institute of Mineral Resources named after N.M. Fedorovsky (S.V. Kordyukov, Moscow).

Seven kilometers along the strike of the Gorodishche Formation to the north of the Osipovka occurrence on the right side of the Sanarka River, 0.5 km downstream from the Belokamenka settlement, in silicified and sulfidized graphitic quartzites penetrated by a dyke of plagiogranites (Figure 18b), an average gold content of 0.75 g/t (maximum is 7.7 g/t) and platinum content of 0.57 g/t were obtained from 10 samples, which suggests the presence of a single zone of gold mineralization and recommends it for further prospecting and assessment work. The Osipovka gold and platinum occurrence is the first object identified among the carbonaceous sediments of the Trans-Ural Uplift.

#### 4. Conclusions

The above results on the study of carbonaceous sediments of the Southern Urals indicate very high prospects for discovering gold mineralization in them. The framing of Larino and Beloretsk granite–gneiss domes and the western contacts of the Suunduk and Nizhnesanarka granite massifs are mainly made up of carbonaceous sediments, saturated with magmatic rocks of different compositions and ages and subjected to moderate metamorphism. These are the first-priority objects for prospecting. In this regard, the confinement of gold occurrences to the outer high-temperature subfacies of the greenschist facies serves as a very important prospecting criterion. The Larino, Otnurok, Amur, and Osipovo gold occurrences discovered here confirm that our conclusions are correct. Carbonaceous sediments located among the rocks of the ophiolite formation are also of great interest. The high degree of their dislocation, silicification, and sulfidization, found, in particular, within the Siratur and Chernoe Ozero occurrences, can be considered an additional criterion for the prospects of black shale formations.

In general, gold–PGE specialization is observed in the carbonaceous formations of the Southern Urals. Their contents are abnormally high and reach 25 g/t for Au, 0.75 g/t for Pt, and 1.8 g/t for Pd. The Pd/Pt ratio is 5–10 units on average but can reach 100 units in altered carbonaceous shales, which indicates the significant mobility of PGE in metasomatic processes. The spatial combination of gold and PGE mineralization is not unique and is typical of many black shale complexes of the world. A distinctive feature of the South Ural black shales is the absence of other platinum group metals. Significant contents of Os, Ir, Rh, and Ru were not detected in any of the 150 analyzed samples.

The presented data indicate a high gold and MPG potential of the carbonaceous deposits of the Southern Urals and are a good basis for further exploration work.

**Author Contributions:** Investigation, fieldwork, sample preparation, writing—original draft preparation, and writing—review and editing, A.V.S. and M.A.R.; study of samples on an electron microscope, M.A.R.; project administration and funding acquisition, A.V.S. All authors have read and agreed to the published version of the manuscript.

**Funding:** The study was funded by the Russian Science Foundation, grant No. 23-27-00265, accessed on 13 January 2023, <https://rscf.ru/en/project/23-27-00265/>.

**Data Availability Statement:** The data presented in this study are available upon request from the corresponding author.

**Acknowledgments:** The authors are grateful to the anonymous reviewers for their very detailed and constructive reviews, which helped us greatly to improve the paper.

**Conflicts of Interest:** The authors declare no conflicts of interest.

#### References

1. Korobeynikov, A.F. Mineralogy of noble metals of non-traditional gold-platinoid ores in black shale formations. In *Platinum of Russia. Problems of Development of Mineral Resource Base of Platinum Metals in the 21st Century*; Geoinformimark: Moscow, Russia, 1999; pp. 40–51. (In Russian)
2. Marakushev, A.A. Black shale formations as an indicator of periods of catastrophic development of the Earth. In *Platinum of Russia. Problems of Development of Mineral Resource Base of Platinum Metals in the 21st Century*; Geoinformimark: Moscow, Russia, 1999; pp. 183–194. (In Russian)
3. Wood, B.L.; Popov, N.P. The giant Sukhoi Log deposit, Siberia. *Russ. Geol. Geophys.* **2006**, *47*, 315–341.
4. Sazonov, V.N.; Koroteev, V.A.; Ogorodnikov, V.N.; Polenov, Y.A.; Velikanov, A.Y. Gold in “black shales” of the Urals. *Litosfera* **2011**, *4*, 70–92. (In Russian)
5. Ermolaev, N.P.; Sozinov, N.A. *Stratiform Mineralization in Black Shales*; Nauka: Moscow, Russia, 1986; 244p. (In Russian)
6. Shumilova, T.G.; Shevchuk, S.S.; Isayenko, S.I. Metal concentrations and carbonaceous matter in the black shale type rocks of the Urals. *Dokl. Earth Sci.* **2016**, *469*, 695–698. [[CrossRef](#)]
7. Bespayev, K.A.; Parilov, Y.S.; Rodnova, V.I.; Mukaeva, A.E. On the assessment of gold content in South-Eastern Kazakhstan. *Geol. Subsoil Prot.* **2017**, *2*, 4–15. (In Russian)

8. Ivanov, A.I. The role played by metamorphic transformation conditions of carbonaceous carbonate-terrigenous deposits for gold mineralization formation at various stages of collisional epoch of Baikal-Patom metallogenic province development. *Otechestvennaya Geol.* **2017**, *4*, 3–23. (In Russian)
9. Groves, D.I.; Goldfarb, R.J.; Robert, F.; Hart, C.J.R. Gold deposits in metamorphic belts: Overview of current understanding, outstanding problems, future research, and significance. *Econ. Geol.* **2003**, *98*, 1–29. [[CrossRef](#)]
10. Laranjeira, V.; Ribeiro, J.; Moreira, N.; Nogueira, P.; Flores, D. Geochemistry of Precambrian black shales from Ossa-Morena Zone (Portugal): Depositional environment and possible source of metals. *J. Iber. Geol.* **2023**, *49*, 1–19. [[CrossRef](#)]
11. Groves, D.I.; Santosh, M.; Goldfarb, R.J.; Zhang, L. Structural geometry of orogenic gold deposits: Implications for exploration of world-class and giant deposits. *Geosci. Front.* **2018**, *9*, 1163–1177. [[CrossRef](#)]
12. Gadd, M.G.; Peter, J.M.; Jackson, S.E.; Yang, Z.; Petts, D. Platinum, Pd, Mo, Au and Re department in hyper-enriched black shale Ni-Zn-Mo-PGE mineralization, Peel River, Yukon, Canada. *Ore Geol. Rev.* **2019**, *107*, 600–614. [[CrossRef](#)]
13. Nesbitt, B.E.; Muehlenbachs, K. Origins and movement of fluids during deformation and metamorphism in the Canadian Cordillera. *Science* **1989**, *245*, 733–736. [[CrossRef](#)]
14. Goldfarb, R.J.; Groves, D.I.; Cardoll, S. Orogenic Au and geologic time: A global synthesis. *Ore Geol. Rev.* **2001**, *18*, 1–75. [[CrossRef](#)]
15. Bortnikov, N.S. Geochemistry and origin of the ore-forming fluids in hydrothermal-magmatic systems in tectonically active zones. *Geol. Ore Depos.* **2006**, *48*, 1–22. [[CrossRef](#)]
16. Goryachev, N.A.; Pirajno, F. Gold deposits and gold metallogeny of Far East Russia. *Ore Geol. Rev.* **2014**, *59*, 123–151. [[CrossRef](#)]
17. Groves, D.I.; Goldfarb, R.J.; Gebre-Mariam, M.; Hagemann, S.G.; Robert, F. Orogenic gold deposits: A proposed classification in the context of their crustal distribution and relationship to other gold deposit types. *Ore Geol. Rev.* **1998**, *13*, 7–27. [[CrossRef](#)]
18. Goldfarb, R.J.; Groves, D.I. Orogenic gold: Common or evolving fluid and metal sources through time. *Lithos* **2015**, *233*, 2–26. [[CrossRef](#)]
19. Rundkvist, D.V.; Ryakhovskii, V.M.; Mironov, Y.V.; Pustovoi, A.A. On the Trends and Rhythmicity of the Global Evolution of the Magmatism of the World Ocean. *Dokl. Earth Sci.* **1998**, *363*, 523–526.
20. Konstantinov, M.M. Gold ore deposits of the Carlin type and criteria for their identification. *Rudy Met.* **2000**, *1*, 70–76. (In Russian)
21. Konstantinov, M.M.; Nekrasov, E.M.; Sidorov, A.A.; Struzhkov, S.F. *Gold Ore Giants of Russia and the World*; Nauchnyy Mir: Moscow, Russia, 2000; 272p. (In Russian)
22. Laverov, N.P.; Prokof'ev, V.Y.; Distler, V.V.; Yudovskaya, M.A.; Spiridonov, A.M.; Grebeshchikova, V.I.; Matel, N.L. New data on conditions of ore deposition and composition of ore-forming fluids in the Sukhoy Log gold-platinum deposit. *Dokl. Earth Sci.* **2000**, *371*, 357–361.
23. Bortnikov, N.S.; Gamyarin, G.N.; Vikent'eva, O.V.; Prokof'ev, V.Y.; Alpatov, V.A.; Bakharev, A.G. Fluid Composition and Origin in the Hydrothermal System of the Nezhdaninsky Gold Deposit, Sakha (Yakutia), Russia. *Geol. Ore Depos.* **2007**, *49*, 87–128. [[CrossRef](#)]
24. Goryachev, N.A.; Vikenteva, O.V.; Bortnikov, N.S.; Prokof'ev, V.Y.; Alpatov, V.A.; Golub, V.V. The world-class Natalka gold deposit, northeast Russia: REE patterns, fluid inclusions, stable oxygen isotopes, and formation conditions of ore. *Geol. Ore Depos.* **2008**, *50*, 362–390. [[CrossRef](#)]
25. Ridley, J.R.; Diamond, L.W. Fluid chemistry of orogenic lode gold deposits and implications for genetic models. In *Gold in 2000. Reviews in Economic Geology*; Hagemann, S.G., Brown, P.E., Eds.; Society of Economic Geologists: Denver, CO, USA, 2000; Volume 13, pp. 141–162. [[CrossRef](#)]
26. Kempe, U.; Belyatsky, B.; Krymsky, R.; Kremenetsky, A.; Ivanov, P. Sm–Nd and Sr isotope systematics of scheelite from the giant Au(–W) deposit Muruntau (Uzbekistan): Implications for the age and sources of Au mineralization. *Min. Dep.* **2001**, *36*, 379–392. [[CrossRef](#)]
27. Bortnikov, N.S.; Simonov, V.A.; Bogdanov, Y.A. Fluid inclusions in minerals from modern sulfide edifices: Physicochemical conditions of formation and evolution of fluids. *Geol. Ore Depos.* **2004**, *46*, 64–75.
28. Chernyshev, I.V.; Filimonova, L.G.; Chugaev, A.V.; Pushkarev, Y.D. Sources of Ore Matter of the Dukat Gold-Silver Deposit (Northeastern Russia): Data from Pb, Sr, and Nd Isotope Studies. *Geol. Ore Depos.* **2005**, *47*, 269–282.
29. Naumov, G.B.; Vlasov, B.P.; Mironov, O.F. Towards the question of the movement of hydrothermal solutions: The case of the Schlema-Alberoda vein deposit. *Geol. Ore Depos.* **2014**, *56*, 346–356. [[CrossRef](#)]
30. Vysotskiy, S.V.; Khanchuk, A.I.; Velivetskaya, T.A.; Ignatiev, A.V.; Aseeva, A.V.; Nesterova, N.S.; Karpenko, A.A.; Ruslan, A.V. New Evidence of the Organic Origin of Carbonaceous Matter in Archean Banded Iron Formation of the Kostomuksha Greenstone Belt of Karelia, Russia. *Dokl. Earth Sci.* **2024**, *514*, 281–286. [[CrossRef](#)]
31. Buryak, V.A. *Metamorphism and Ore Formation*; Nedra: Moscow, Russia, 1982; 256p. (In Russian)
32. Buryak, V.A.; Goncharov, V.I.; Goryachev, N.A. Evolutionary series of large deposits of gold and platinum group metals in carbonaceous sequences. *Dokl. Earth Sci.* **2002**, *387*, 1007–1009.
33. Yakubchuk, A.; Shatov, V.V.; Kirwin, D.; Edwards, A.; Badarch, G.; Buryak, V.A. Gold and base metal metallogeny of the Central Asian orogenic, supercollage. In *100th Anniversary Volume*; Hedenquist, J.W., Thompson, J.F.H., Goldfarb, R.J., Richards, J.P., Eds.; Society of Economic Geologists: Denver, CO, USA, 2005; pp. 1035–1068.
34. Vilor, N.V. Gold in black shales. *Geochem. Int.* **1983**, *20*, 167–177.

35. Dobretsov, N.L.; Krivtsov, A.I. Models of magmatic-hydrothermal and metamorphic-hydrothermal ore accumulation and criteria for their distinction. In *Criteria for Distinguishing Metamorphic and Magmatic Hydrothermal Deposits*; Nauka: Novosibirsk, Russia, 1985; pp. 5–14. (In Russian)
36. Rykus, M.V.; Snachev, V.I. *Gold of the Western Slope of the Southern Urals*; Ufa Scientific Center RAS: Ufa, Russia, 1999; 170p. (In Russian)
37. Kribek, B. Metallogeny, structural, lithological and time controls of ore deposition in anoxic environments. *Miner. Depos.* **1991**, *26*, 122–131. [[CrossRef](#)]
38. Hutchinson, R.W. A multi-stage, multi-process genetic hypothesis for greenstonehosted gold lodes. *Ore Geol. Rev.* **1993**, *8*, 349–382. [[CrossRef](#)]
39. Cooke, D.R.; Bull, S.W.; Large, R.R.; McGoldrick, P.J. The importance of oxidized brines for the formation of Australian Proterozoic stratiform sediment-hosted Pb-Zn (sedex) deposits. *Econ. Geol.* **2000**, *95*, 1–18. [[CrossRef](#)]
40. Emsbo, P.; Hofstra, A.H.; Lauha, E.A.; Griffin, G.L.; Hutchinson, R.W. Origin of high-grade gold ore, source of ore fluid components, and genesis of the Meikle and neighboring Carlin-type deposits, northern Carlin Trend, Nevada. *Econ. Geol.* **2003**, *98*, 1069–1105. [[CrossRef](#)]
41. Cline, J.S.; Hofstra, A.; Munteau, J.; Tosdal, D.; Hickey, K. Carlin-type gold deposits in Nevada: Critical geologic characteristics and viable models. In *100th Anniversary Volume*; Hedenquist, J.W., Thompson, J.F.H., Goldfarb, R.J., Richards, J.P., Eds.; Society of Economic Geologists: Denver, CO, USA, 2005; pp. 451–484. [[CrossRef](#)]
42. Large, R.R.; Maslennikov, V.; Robert, F.; Danyushevsky, L.V.; Chang, Z. Multistage sedimentary and metamorphic origin of pyrite and gold in the giant Sukhoi Log deposit, Lena gold province, Russia. *Econ. Geol.* **2007**, *102*, 1233–1267. [[CrossRef](#)]
43. Large, R.R.; Danyushevsky, L.V.; Hollit, C.; Maslennikov, V.; Meffre, S.; Gilbert, S.; Bull, S.; Scott, R.; Emsbo, P.; Thomas, H.; et al. Gold and trace element zonation in pyrite using a laser imaging technique: Implications for the timing of gold in orogenic and Carlin-style sedimenthosted deposits. *Econ. Geol.* **2009**, *104*, 635–668. [[CrossRef](#)]
44. Large, R.R.; Bull, S.W.; Maslennikov, V.V. A Carbonaceous Sedimentary Source-Rock Model for Carlin-Type and Orogenic Gold Deposits. *Econ. Geol.* **2011**, *106*, 331–358. [[CrossRef](#)]
45. Munteau, J.; Cline, J.; Simon, A.; Long, A. Magmatic-hydrothermal origin of Nevada’s Carlin-type gold deposits. *Nat. Geosci.* **2011**, *4*, 122–127. [[CrossRef](#)]
46. Zhang, H.D.; Liu, J.C.; Fayek, M. Multistage mineralization in the Haoyaoerhudong gold deposit, Central Asian Orogenic Belt: Constraints from the sedimentary-diagenetic and hydrothermal sulfides and gold. *Geosci. Front.* **2021**, *12*, 587–604. [[CrossRef](#)]
47. Korobeinikov, A.F. Gold distribution peculiarities in the rocks of black shale formation. *Geokhimiya* **1985**, *12*, 1747–1757. (In Russian)
48. Buryak, V.A. Sources of gold and associated components in gold deposits hosted in carbonaceous strata. *Geol. Rudn. Mestorozhdeniy* **1986**, *28*, 31–43. (In Russian)
49. Fleet, M.E.; Chryssoulis, S.L.; Maclean, P.J.; Davidson, R.; Weisener, G.G. Arsenian pyrite from gold deposits—Au and As distribution investigated by SIMS and EMP, and color staining and surface oxidation by XPS and LIMS. *Can. Mineral.* **1993**, *31*, 1–17.
50. Nekrasov, I.Y. *Geochemistry, Mineralogy and Genesis of Gold Deposits*, 1st ed.; Routledge: London, UK, 1996; 329p. [[CrossRef](#)]
51. Kesler, S.E.; Fortuna, J.; Ye, Z.; Alt, J.C.; Core, D.P.; Zohar, P.; Borhauer, J.; Chryssoulis, S.L. Evaluation of the role of sulfidation in deposition of gold, Screamer section of the Betze-Post Carlin-type deposit, Nevada. *Econ. Geol.* **2003**, *98*, 1137–1157. [[CrossRef](#)]
52. Plyusnina, L.P.; Kuz’mina, T.V.; Avchenko, O.V. Modeling of gold sorption on carbonaceous matter at 20–500 °C and 1 kbar. *Geochem. Int.* **2004**, *42*, 755–763. [[CrossRef](#)]
53. Johnson, P.R.; Zoheir, B.A.; Ghebreab, W.; Stern, R.J.; Barrie, C.T.; Hamer, R.D. Gold-bearing volcanogenic massive sulfides and orogenic-gold deposits in the Nubian Shield. *S. Afr. J. Geol.* **2017**, *120*, 63–76. [[CrossRef](#)]
54. Zoheir, B.A.; Johnson, P.R.; Goldfarb, R.J.; Klemm, D.D. Orogenic gold in the Egyptian Eastern Desert: Widespread gold mineralization in the late stages of Neoproterozoic orogeny. *Gondwana Res.* **2019**, *75*, 184–217. [[CrossRef](#)]
55. Razvozzhaeva, E.A.; Prokof’ev, V.Y.; Spiridonov, A.M.; Martikhaev, D.K.; Prokopchuk, S.I. Precious Metals and Carbonaceous Substance in Ores of the Sukhoi Log Deposit (Eastern Siberia, Russia). *Geol. Ore Depos.* **2002**, *44*, 103–110.
56. Razvozzhaeva, E.A.; Budyak, A.E.; Prokopchuk, S.I. Sorption capacity of insoluble carbonaceous matter in black shales affected by regional metamorphism: Baikal-Patom highland. *Geochem. Int.* **2013**, *51*, 83–86. [[CrossRef](#)]
57. Razvozzhaeva, E.A.; Nemerov, V.K.; Spiridonov, A.M.; Prokopchuk, S.I. Carbonaceous substance of the Sukhoi Log gold deposit (East Siberia). *Rus. Geol. Geophys.* **2008**, *49*, 371–377. [[CrossRef](#)]
58. Yudovskaya, M.A.; Distler, V.V.; Prokofiev, V.Y.; Akinfiev, N.N. Gold mineralisation and orogenic metamorphism in the Lena province of Siberia as assessed from Chertovo Koryto and Sukhoi Log deposits. *Geosci. Front.* **2016**, *7*, 453–481. [[CrossRef](#)]
59. Snachev, A.V.; Snachev, V.I.; Rykus, M.V.; Saveliev, D.E.; Bazhin, E.A.; Ardislamov, F.R. *Geology, Petrogeochemistry and Ore Content of Carbonaceous Deposits of the Southern Urals*; Design Poligraf Service: Ufa, Russia, 2012; 208p. (In Russian)
60. Snachev, A.V.; Rykus, M.V.; Snachev, M.V.; Romanovskaya, M.A. A model for the genesis of gold mineralization in carbonaceous schists of the Southern Urals. *Mosc. Univ. Geol. Bull.* **2013**, *68*, 108–117. [[CrossRef](#)]
61. Puchkov, V.N. General features relating to the occurrence of mineral deposits in the Urals: What, where, when and why. *Ore Geol. Rev.* **2017**, *85*, 4–29. [[CrossRef](#)]
62. Kovalev, S.G. Intricately dislocated carbonaceous rocks on the Western slope of the Southern Urals. *Dokl. Earth Sci.* **2004**, *396*, 496–499.

63. Snachev, A.V.; Snachev, V.I.; Ardislamov, F.R. Forecast Reserves of Gold in Komarovskian Carbon Sediments of Beloretsky Metamorphic Complex (The South Urals). *Georesursy* **2015**, *4*, 99–104. [[CrossRef](#)]
64. Snachev, A.V.; Snachev, V.I.; Romanovskaya, M.A. The geology, petrogeochemistry, and ore content of carbonaceous deposits from the Larinsky dome (South Urals). *Mosc. Univ. Geol. Bull.* **2015**, *70*, 131–140. [[CrossRef](#)]
65. Snachev, A.V.; Nugumanova, J.N.; Saveliev, D.E. Ore prospects of carbonaceous deposits of the Maksyutovo complex (Uraltau zone). *Geol. Vestn.* **2019**, *1*, 55–67. [[CrossRef](#)]
66. Volchenko, Y.A.; Koroteev, V.A.; Zoloev, K.K.; Neustroeva, I.I. Platinum metals and gold in carbonaceous black shale strata of the Urals. In *Geology and Mineral Resources of the Western Urals*; Perm State National Research University: Perm, Russia, 2001; p. 104. (In Russian)
67. Maslov, A.V.; Kovalev, S.G.; Gareev, E.Z. Riphean low-carbonaceous shales of the South Urals in the context of formation of Large Igneous Provinces. *Geochem. Int.* **2017**, *7*, 608–620. [[CrossRef](#)]
68. Khitrov, V.G.; Belousov, G.E.; Sychkova, V.A. Spectrochemical analysis procedure for natural and industrial materials on platinum metals. *J. Appl. Spectrosc.* **1980**, *32*, 429–432. [[CrossRef](#)]
69. Distler, V.V.; Mitrofanov, G.L.; Nemerov, V.K.; Kovalenker, V.A.; Mokhov, A.V.; Semeikina, L.K.; Yudovskaya, M.A. Modes of occurrence of the platinum group elements and their origin in the Sukhoi Log Gold Deposit (Russia). *Geol. Ore Depos.* **1996**, *38*, 413–428.
70. Distler, V.V.; Yudovskaya, M.A.; Mokhov, A.V.; Trubkin, N.V.; Razvozzhaeva, E.A.; Mitrofanov, G.L.; Nemerov, V.K. New data on PGE mineralization in gold ores of the Sukhoi Log deposit, Lensk gold-bearing district, Russia. *Dokl. Earth Sci.* **2003**, *393*, 1265–1267.
71. Distler, V.V.; Yudovskaya, M.A.; Mitrofanov, G.L.; Prokof'ev, V.V.; Lishnevsii, E.N. Geology, composition, and genesis of the Sukhoi Log noble metals deposit, Russia. *Ore Geol. Rev.* **2004**, *24*, 7–44. [[CrossRef](#)]
72. Kolosova, L.P.; Aladyshkina, A.E.; Ushinskaya, L.A.; Kopylova, T.N. Simultaneous atomic emission determination of Pt, Pd, Rh, Ir, Ru, Os, Au in assay concentrate. *J. Anal. Chem.* **1991**, *46*, 1386–1390.
73. Battaini, P.; Bemporad, E.; De Felicis, D. The fire assay reloaded. *Gold Bull.* **2014**, *47*, 9–20. [[CrossRef](#)]
74. Mandrugina, A.V.; Sedelnikov, G.V.; Kuznetsov, A.P.; Puchkova, T.V.; Serebryany, B.L.; Simakova, L.G.; Guma, V.I. Modern techniques and methods of the geological materials analysis for precious and base metals. *Rudy Met.* **2015**, *1*, 64–73. (In Russian)
75. Knyazev, Y.G.; Knyazeva, O.Y.; Snachev, V.I.; Zhdanov, A.V.; Karimov, T.R.; Aidarov, E.M.; Masagutov, R.K.; Arslanova, E.R. *State Geological Map of the Russian Federation. Scale 1:1000000 (3rd Generation). Ural Series. Sheet N-40 (Ufa). Explanatory Letter*; FGBU VSEGEI: St. Petersburg, Russia, 2013; 512p. (In Russian)
76. Alekseev, A.A.; Kovalev, S.G.; Timofeeva, E.A. *Beloretsk Metamorphic Complex*; Design Poligraph Service: Ufa, Russia, 2009; 210p. (In Russian)
77. Krasnobaev, A.A.; Kozlov, V.I.; Puchkov, V.N.; Rodionov, N.V.; Nekhorosheva, A.G.; Kiseeva, K.N. The Akhmerovo granite massif: A proxy of mesoproterozoic intrusive magmatism in the Southern Urals. *Dokl. Earth Sci.* **2008**, *418*, 103–108. [[CrossRef](#)]
78. Snachev, A.V.; Puchkov, V.N. First findings of palladium-gold-REE ore mineralization in precambrian carbonaceous shales on the western slope of the Southern urals. *Dokl. Earth Sci.* **2010**, *433*, 866–869. [[CrossRef](#)]
79. Kovalev, S.G.; Michurin, S.V. Geochemical features of carbonaceous rocks on the western slope of the Southern Urals. *Lithol. Miner. Resour.* **2005**, *40*, 245–253. [[CrossRef](#)]
80. Michurin, S.V.; Sharipova, A.A.; Krupenin, M.T.; Zamyatin, D.A.; Musina, A.M.; Popov, V.A. Sulfide mineralization, native gold and its geochemical connections in the Riphean deposits of the Avzyan ore-bearing region (the Southern Urals). *Lithosphere* **2018**, *18*, 61–81. [[CrossRef](#)]
81. Palenova, E.E.; Novoselov, K.A.; Belogub, E.V.; Blinov, I.A.; Grigor'eva, S.D. Mineralogy of alluvial sediments of Avzyan gold region (the Southern Urals). *Litosfera* **2018**, *18*, 459–474. (In Russian) [[CrossRef](#)]
82. Kovalev, S.G.; Michurin, S.V.; Maslov, A.V.; Sharipova, A.A. First data on the geochemistry of rare earth elements and platinoids in the rocks of the gold mining deposit Ulyuk-Bar (the Southern Urals). *Litosfera* **2020**, *20*, 573–591. [[CrossRef](#)]
83. Michurin, S.V.; Sharipova, A.A. The first finds of copper gold in the Riphean deposits of the Bashkir meganticlinorium (Southern Urals). *Bull. Voronezh State Tech. Univ. Ser. Geol.* **2022**, *3*, 52–56. (In Russian) [[CrossRef](#)]
84. Nikonov, V.N.; Vysotsky, I.V.; Menshikov, V.G.; Boykov, G.V. Technogenic resources of the Republic of Bashkortostan—A large-scale base for production expansion. In *Mineral Resource Base of the Republic of Bashkortostan: Reality and Prospects, Proceedings of the Republic Scientific and Practical Conference, Vitebsk, Belarus, 28 October 2016*; Tau: Ufa, Russia, 2002; pp. 540–555. (In Russian)
85. Kovalev, S.G.; Salikhov, D.N.; Puchkov, V.N. *Minerals of the Republic of Bashkortostan (Metals)*; Alfa-reklama: Ufa, Russia, 2016; 554p. (In Russian)
86. Snachev, A.V.; Kazakov, P.V.; Rassomakhin, M.A.; Islamov, R.R. Genetic Relationship of the “From Primary to Placer” System Using the Example of the Gorny Priisk Gold Deposit (Avzyan Ore-Placer Field, Southern Urals). *Eurasian Min.* **2025**, *in press*.
87. Osovetskiy, B.M. *Natural Nanogold*; Perm University: Perm, Russia, 2013; 176p. (In Russian)
88. Kovalev, S.G.; Vyssotskii, I.V.; Michurin, S.V.; Kovalev, S.S. Geology, mineralogy, and metallogenic specialization of the carbon-bearing sequences of the Uluelga-Kudashman Zone (western slope of the southern Urals). *Litosfera* **2013**, *3*, 67–88. (In Russian)
89. Rykus, M.V.; Snachev, V.I.; Nasibullin, R.A.; Rykus, N.G.; Savelyev, D.E. *Sedimentation, Magmatism and Ore-Bearing Capacity of the Northern Part of the Uraltau Zone*; Bashkir State University: Ufa, Russia, 2002; 268p. (In Russian)

90. Saveliev, D.E.; Kazakov, P.V.; Bazhin, E.A. Placer and orogenic gold mineralization prospects of the northern part of the Zilairsky megasynclorium, the Southern Urals. *Rudy Met.* **2016**, *2*, 44–50. (In Russian)
91. Snachev, A.V.; Snachev, V.I. Prospects of carbonaceous deposits of Novousmanovsky area on rhenium, tungsten, molybdenum (Uraltau zone). *Geol. Vestn.* **2018**, *2*, 68–78. (In Russian) [[CrossRef](#)]
92. Znamensky, S.E. The Late Paleozoic structural evolution of the Magnitogorsk Megazone in the southern Urals. *Dokl. Earth Sci.* **2008**, *420*, 547–550. [[CrossRef](#)]
93. Znamensky, S.E.; Znamenskaya, N.M. Structural Control and Prospects of Searches of Gold Mineralization in the Nuralino-Voznesensko-Buibinsky Fault Zone (the Southern Urals). *Georesursy* **2016**, *18*, 68–74. [[CrossRef](#)]
94. Snachev, A.V.; Latypov, F.F.; Snachev, V.I.; Rassomakhin, M.A.; Koshchug, D.G.; Vyatkin, S.V. The Siratur Gold Deposit in Carbonaceous Rocks of an Ophiolite Association, South Urals. *Mosc. Univ. Geol. Bull.* **2020**, *75*, 609–615. [[CrossRef](#)]
95. Nurieva, K.R.; Snachev, A.V.; Latypov, F.F.; Gataullin, R.A.; Rassomakhin, M.A. Geology of the Golenkie Gorki gold show (Siraturskoye ore field, the Southern Urals). *Geol. Vestn.* **2022**, *3*, 53–64. (In Russian) [[CrossRef](#)]
96. Maslov, V.A.; Artyushkova, O.V. *Stratigraphy of Paleozoic Formations of the Uchalinsky District of Bashkiria*; Institute of Geology UfSC RAS: Ufa, Russia, 2000; 140p. (In Russian)
97. Anfilogov, V.N.; Krasnobaev, A.A.; Valizer, P.M. The age of ultramafic rocks of the main Ural Fault. *Dokl. Earth Sci.* **2018**, *482*, 1249–1251. [[CrossRef](#)]
98. Krasnobaev, A.A.; Rusin, A.I.; Valizer, P.M.; Likhanov, I.I. Zirconology of the Lherzolite Block of the Nurali Massif (South Urals). *Russ. Geol. Geophys.* **2019**, *60*, 435–446. [[CrossRef](#)]
99. Aulov, B.N.; Vladimirtseva, Y.A.; Gvozdik, N.I.; Korolkova, Z.G.; Levin, F.D.; Lipaeva, A.V.; Potashova, M.N.; Samozvantsev, V.A. *State Geological Map of the Russian Federation. Scale 1:200,000. Second Edition. South Ural Series. Sheet N-40-XII—Zlatoust. Explanatory Note*; VSEGEI: Moscow, Russia, 2015; 365p. (In Russian)
100. Snachev, A.V. Geology and sedimentation conditions of carbonaceous deposits of the Siratur ore field. *Vestn. Akad. Nauk. RB* **2019**, *32*, 15–25. (In Russian) [[CrossRef](#)]
101. Snachyov, A.V.; Kuznetsov, N.S.; Snachyov, V.I. The Chernoe Ozero gold occurrence in carbonaceous deposits of the ophiolite association: The first object of such a type in the Southern Urals. *Dokl. Earth Sci.* **2011**, *439*, 906–908. [[CrossRef](#)]
102. Murzin, V.V.; Chudnenko, K.V.; Palyanova, G.A.; Varlamov, D.A.; Naumov, E.A.; Pirajno, F. Physicochemical model for the genesis of Cu-Ag-Au-Hg solid solutions and intermetallics in the rodingites of the Zolotaya Gora gold deposit (Urals, Russia). *Ore Geol. Rev.* **2018**, *93*, 81–97. [[CrossRef](#)]
103. Murzin, V.; Chudnenko, K.; Palyanova, G.; Kissin, A.; Varlamov, D. Physicochemical Model of Formation of Gold-Bearing Magnetite-Chlorite-Carbonate Rocks at the Karabash Ultramafic Massif (Southern Urals, Russia). *Minerals* **2018**, *8*, 306. [[CrossRef](#)]
104. Seravkin, I.B.; Snachev, V.I. Stratiform base-metal deposits in the eastern province of the Southern Urals, Russia. *Geol. Ore Depos.* **2012**, *54*, 209–218. [[CrossRef](#)]
105. Snachev, M.V.; Snachev, A.V.; Puchkov, V.N. New data on the structure of the Amur stratiform deposit (Southern Urals). *Dokl. Earth Sci.* **2015**, *463*, 778–781. [[CrossRef](#)]
106. Snachev, A.V.; Snachev, M.V. Ore Mineralization of the Amur Stratiform Zinc Deposit (Southern Urals). *Dokl. Earth Sci.* **2012**, *444*, 711–714. [[CrossRef](#)]
107. Tevelev, A.V.; Kosheleva, I.A.; Tevelev, A.V.; Pravikova, N.V.; Furina, M.A.; Yakovishina, E.V.; Lubnina, N.V. *State Geological Map of the Russian Federation. Scale 1:200000 (2nd Generation). South Ural Series. Sheet N-40-XXXVI (Quarkenno). Explanatory Letter*; VSEGEI: Moscow, Russia, 2018; 226p. (In Russian)
108. Shirobokova, T.I. *Stratiform Polymetallic and Barite Mineralization of the Urals*; Ural Branch of the USSR Academy of Sciences: Sverdlovsk, Russia, 1992; 141p. (In Russian)
109. Novoselov, K.A.; Belogub, E.V. Gold and silver in sulfide ores of the Amur zinc deposit. In *Mineralogy of the Urals, Proceedings of the VI All-Russian Conference, Sevastopol, Crimea, 22–29 August 2021*; Institute of Mineralogy UB of RAS: Miass, Russia, 2011; pp. 118–122. (In Russian)
110. Plotinskaya, O.Y.; Novoselov, K.A.; Seltsmann, R. Mineralogy of Precious Metals in Ores of the Biksizak Base-Metal Deposit, South Urals, Russia. *Geol. Ore Depos.* **2020**, *62*, 439–456. [[CrossRef](#)]
111. Blinov, I.A. Native metals, selenides, halides and associated minerals from brown iron ore of the Amur and Verkhne-Arshinsky deposits (South Ural). *Litosfera* **2015**, *1*, 65–74. (In Russian)
112. Artyushkova, O.V.; Kurilenko, A.V.; Yakupov, R.R.; Maslov, V.A.; Zianberdin, R.I. New data on the age of the Amur pyrite-sphalerite copper pyrite deposit (South Urals). *Geol. Sb.* **2007**, *6*, 38–39. (In Russian)
113. Snachev, A.V. Carbonaceous matter of black shales of the Amur series (South Urals). *Neftegazov. Delo* **2022**, *20*, 6–18. (In Russian) [[CrossRef](#)]
114. Puzhakov, B.A.; Shokh, V.D.; Schulkina, N.E.; Shchulkin, E.P.; Dolgova, O.Y.; Orlov, M.V.; Popova, T.A.; Tarelkina, E.A.; Ivanov, A.V. *State Geological Map of the Russian Federation. Scale 1:200 000 (2nd ed.) South Ural Series. Sheet N-41-XIII (Plast). Explanatory Note*; VSEGEI: Moscow, Russia, 2018; 205p. (In Russian)
115. Zhdanov, A.V.; Obodov, V.A.; Makariiev, L.B.; Matyushkov, A.D.; Molchanova, E.V.; Stromov, V.A. *State Geological Map of the Russian Federation. Scale 1:200 000 (2nd ed.) South Ural Series. Sheet N-40-XVIII (Uchaly). Explanatory Note*; VSEGEI: Moscow, Russia, 2018; 386p. (In Russian)

116. Snachev, V.I.; Snachev, A.V.; Prokofiev, V.Y. Physicochemical conditions of the formation of the Larino granite-gneiss dome (South Ural). *Georesursy* **2022**, *24*, 74–83. [[CrossRef](#)]
117. Puchkov, V.N.; Ivanov, K.S. On the stratigraphy of black shale strata in the eastern Urals. In *Yezhegodnik-1988*; IGIg UFAN USSR: Sverdlovsk, Russia, 1989; pp. 4–7. (In Russian)
118. Korekina, M.A.; Shanina, S.N.; Savichev, A.N.; Pankrushina, E.A.; Shtenberg, M.V.; Morozov, P.S.; Artemiev, D.A. Water-Containing Defects in Various Deformed Milky-White Vein Quartz of the Larino Deposit (South Urals). *Russ. Geol. Geophys.* **2024**, *65*, 899–909. [[CrossRef](#)]
119. Artyushkova, O.V.; Mavrinskaya, T.M.; Suyarkova, A.A.; Yakupov, R.R.; Maslov, V.A. New finds of fauna in Paleozoic Zauralye. *Geol. Sb.* **2011**, *9*, 32–35. (In Russian)
120. Snachev, A.V.; Shchulkin, E.P. Geological structure and gold-bearing carbonaceous deposits of mount Tetechnaya (South Ural). *Bull. Perm Univ. Geol.* **2018**, *17*, 52–60. [[CrossRef](#)]
121. Snachev, A.V.; Snachev, V.I.; Rassomakhin, M.A.; Kolomoets, A.V. Carbonaceous shales of the Kamensk block: Geology and ore content (South Urals). *Gorn. Zhurnal* **2020**, *2*, 24–29. [[CrossRef](#)]
122. Grabezhev, A.I.; Ronkin, Y.L.; Puchkov, V.N.; Shardakova, G.Y.; Azovskova, O.B.; Gerdes, A. Silurian U–Pb zircon age (LA-ICP-MS) of granitoids from the Zelenodol Cu–porphyry deposit, Southern Urals. *Dokl. Earth Sci.* **2016**, *466*, 92–95. [[CrossRef](#)]
123. Chudnenko, K.V.; Palyanova, G.A. Thermodynamic properties of solid solutions in the Ag–Au–Cu system. *Russ. Geol. Geophys.* **2014**, *55*, 349–360. [[CrossRef](#)]
124. Shatilova, L.V.; Pozdnyakova, N.N.; Krasnov, A.N.; Rogova, O.Y. Typomorphic features of native gold in the placers of the Tarlau area (Southern Urals). *Otechestvennaya Geol.* **2023**, *2*, 27–42. [[CrossRef](#)]
125. Bashirov, V.E.; Kazakov, P.V.; Snachev, A.V.; Gataullin, R.A.; Rassomakhin, M.A. Features of the Tanalyk gold placer and its primary sources (the Baymak ore-placer cluster, Southern Urals). *Geol. Vestn.* **2024**, *1*, 50–63. [[CrossRef](#)]
126. Murzin, V.V.; Malyugin, A.A. *Typomorphism of Gold in the Hypergenesis Zone (Using the Example of the Urals)*; UB USSR Academy of Sciences: Sverdlovsk, Russia, 1987; 96p. (In Russian)
127. Kozin, A.K.; Stepanov, S.Y.; Palamarchuk, R.S.; Shilovskikh, V.V.; Zhdanova, V.S. Mineral Associations of Concentrates from Gold-Bearing Placers of the Miass Placer Zone (South Urals) and Possible Primary Sources of Gold. *Russ. Geol. Geophys.* **2023**, *64*, 1015–1030. [[CrossRef](#)]
128. Shvartsev, S.L.; Dutova, E.M. Hydrochemistry and mobilization of gold in the hypergenesis zone (Kuznetsk Alatau, Russia). *Geol. Ore Depos.* **2001**, *43*, 224–233.
129. Bilibina, T.V.; Bogdanov, Y.V. On the prospects of gold bearing in the Mugodzhzar region. *Geol. Ore Depos.* **1959**, *5*, 104–111.
130. Albov, M.N. *Secondary Zoning of Gold Deposits of the Urals*; Gosgeoltekhizdat: Moscow, Russia, 1960; 215p. (In Russian)
131. Voin, M.I. Features of the structure and mineralization of the Kumak ore field and the methodology for the allocation of enriched intervals in the mineralized zones of crushing. *News Univ. Geol. Explor.* **1966**, *11*, 77–86. (In Russian)
132. Panteleeva, A.V.; Snachev, A.V. *Geology, Petrochemistry and Ore Content of Carbonaceous Deposits of the Kumak Ore Field*; Springer: Cham, Switzerland, 2024; 126p. [[CrossRef](#)]
133. Snachev, A.V.; Kolomoets, A.V.; Rassomakhin, M.A.; Snachev, V.I. Geology and gold content of carbonaceous shale in Baikal mineralization site, Southern Ural. *Eurasian Min.* **2021**, *1*, 8–13. [[CrossRef](#)]
134. Snachev, A.V.; Panteleeva, A.V.; Rassomakhin, M.A. REE minerals in carbonaceous shales of the Kumak gold deposit (South Urals, Russia). *Eurasian Min.* **2023**, *2*, 3–8. [[CrossRef](#)]
135. Arifulov, C.K. Black shale gold deposits of various geological conditions. *Rudy Met.* **2005**, *2*, 9–19. (In Russian)
136. Kolomoets, A.V.; Snachev, A.V.; Rassomakhin, M.A. Gold-tourmaline mineralization in carbonaceous shales of the Kumak deposit (South Ural). *Gorn. Zhurnal* **2020**, *12*, 11–15. [[CrossRef](#)]
137. Lyadskiy, P.V.; Chen-Len-Son, B.I.; Kvasnyuk, L.N.; Alekseeva, G.A.; Olenitsa, T.V.; Manuylov, N.V. *State Geological Map of the Russian Federation. Scale 1:200000. 2nd Edition. Series South Ural. Sheet M-41-VII(XIII) (Svetly). Explanatory Note*; VSEGEI: Moscow, Russia, 2018; 128p. (In Russian)
138. Znamensky, S.E.; Znamenskaya, N.M. Classification of gold deposits of the eastern slope of the Southern Urals. *Geol. Sb.* **2009**, *8*, 177–186. (In Russian)
139. Rudskoy, V.G. The role of metamorphism in the formation of gold ore mineralization of the Kumak ore field. In *Geology of Metamorphic Complexes: Inter-University Scientific Thematic Digest*; Ural Polytechnic Institute: Sverdlovsk, Russia, 1982; pp. 88–94. (In Russian)
140. London, D.; Morgan, G.; Wolf, M. Boron in granitic rocks and their contact aureoles. *Rev. Mineral. Geochem.* **1996**, *33*, 299–330.
141. Baksheev, I.; Prokof'ev, V.Y.; Zaraisky, G.; Chitalin, A.; Yapaskurt, V.; Nikolaev, Y.; Tikhomirov, P.; Nagornaya, E.; Rogacheva, L.; Gorelikova, N.; et al. Tourmaline as a prospecting guide for the porphyry style deposits. *Eur. J. Mineral.* **2012**, *24*, 957–979. [[CrossRef](#)]
142. Jiang, S.J.; Radvanec, M.; Nakamura, E.; Palmer, M.; Kobayashi, K.; Zhao, H.X.; Zhao, K.D. Chemical and boron isotopic variations of tourmaline in the Hnilec granite-related hydrothermal system. Slovakia: Constraints on magmatic and metamorphic fluid evolution. *Lithos* **2008**, *106*, 1–11. [[CrossRef](#)]
143. Hazarika, P.; Mishra, B. Tourmaline as fluid source indicator in the late Archean Hutti orogenic gold deposit. In *Mineral Resources in a Sustainable World*; SGA: Nancy, France, 2015; pp. 465–467.

144. Voudouris, P.; Baksheev, I.A.; Mavrogonatos, C.; Spry, P.G.; Djiba, A.; Bismayer, U.; Papagkikas, K.; Katsara, A. Tourmaline from the Fakos porphyry-epithermal Cu-Mo-Au-Te prospect, Limnos island, Greece: Mineral-chemistry and genetic implications. *Bull. Geol. Soc. Greece* **2019**, *7*, 329–330.
145. Rassomakhin, M.A.; Belogub, E.V.; Novoselov, K.A.; Khvorov, P.V. Tourmalin from late quartz veins of the Murtykty gold deposit, South Ural, Bashkortostan. *Mineralogy* **2020**, *6*, 69–83. (In Russian) [[CrossRef](#)]
146. Kuzhuget, R.V.; Zaikov, V.V.; Lebedev, V.I. The Ulug-Sair gold-tourmaline-quartz deposit, Western Tuva. *Litosfera* **2014**, *2*, 99–114. (In Russian)
147. Gvozdev, V.I.; Grebennikova, A.A.; Vakh, A.S.; Fedoseev, D.G.; Goryachev, N.A. Mineral Evolution during Formation of Gold–Rare-Metal Ores in the Sredne-Golgotay Deposit (Eastern Transbaikalia). *Russ. J. Pac. Geol.* **2020**, *14*, 66–86. [[CrossRef](#)]
148. Cabral, A.R.; Tupinambá, M.; Zeh, A.; Lehmann, B.; Wiedenbeck, M.; Brauns, M.; Kwitko-Ribeiro, R. Platiniferous gold–tourmaline aggregates in the gold–palladium belt of Minas Gerais, Brazil: Implications for regional boron metasomatism. *Miner. Petrol.* **2017**, *111*, 807–819. [[CrossRef](#)]
149. Sokol, E.V.; Kokh, S.N.; Kozmenko, O.A.; Lavrushin, V.Y.; Belogub, E.V.; Khvorov, P.V.; Kikvadze, O. Boron fate in an onshore mud volcanic environment: Case study from the Kerch Peninsula, the Caucasus continental collision zone. *Chem. Geol.* **2019**, *525*, 58–81. [[CrossRef](#)]
150. Snachev, A.V.; Puzhakov, B.A.; Snachev, V.I.; Rykus, M.V. Prospects of carbonaceous deposits in the central part Zauralsk elvation on precious and rare metals. *Electron. Sci. J. Oil Gas Bus.* **2015**, *2*, 123–142. (In Russian) [[CrossRef](#)]

**Disclaimer/Publisher’s Note:** The statements, opinions and data contained in all publications are solely those of the individual author(s) and contributor(s) and not of MDPI and/or the editor(s). MDPI and/or the editor(s) disclaim responsibility for any injury to people or property resulting from any ideas, methods, instructions or products referred to in the content.